



ISAS - INTERNATIONAL SCHOOL FOR ADVANCED STUDIES

Scuola Internazionale Superiore di Studi Avanzati

International School for Advanced Studies

Interaction of massive neutrinos with matter

Thesis submitted for the degree of

“Magister Philosophiæ”

CANDIDATE

Mauro Moretti

SUPERVISORS

Prof. R. Barbieri

Prof S.T. Petcov

October 1991

**SISSA - SCUOLA
INTERNAZIONALE
SUPERIORE
DI STUDI AVANZATI**

TRIESTE
Strada Costiera 11

TRIESTE

Scuola Internazionale Superiore di Studi Avanzati

International School for Advanced Studies

Interaction of massive neutrinos with matter

Thesis submitted for the degree of

“Magister Philosophiæ”

CANDIDATE

Mauro Moretti

SUPERVISORS

Prof. R. Barbieri

Prof S.T. Petcov

October 1991

Introduction

CHAP 1 NEUTRINO OSCILLATION IN VACUUM AND IN MATTER

§1.1 The relevant lagrangian for neutrinos

§1.2 Propagation of a flavour neutrino state in vacuum

§1.3 Relevance of vacuum neutrino oscillation for the solar neutrino problem

§1.4 Matter neutrino oscillation

§1.4.1 The propagation of a neutrino in a dense medium

§1.4.2 Forward scattering amplitudes

§1.4.3 Neutrino evolution equation in matter

§1.4.4 The W. M. S. effect

§1.5 Relevance of neutrino mixing in matter for the solar neutrino problem

CHAP 2 NEUTRINO SPIN PRECESSION IN A COHERENT MAGNETIC FIELD

§2.1 Effective lagrangian accounting for neutrino electromagnetic properties

§2.2 Neutrino evolution equation in a coherent magnetic field

§2.3 The region of parameters relevant for the solar neutrino problem

§2.4 The hybrid models

§2.5 Additional experimental signature of the hybrid models

§2.5.1 Bounds on the $\bar{\nu}_e$ flux from kamiokande II background data

§2.5.2 Hybrid models with large mixing angle and solar $\bar{\nu}_e$ flux

CHAP 3 NEUTRINO OSCILLATION AND MAGNETIC MOMENT TRANSITION IN A MODEL WITH A CONSERVED LEPTON NUMBER

§3.1 The model

§3.2 Flavour oscillations and spin flip in the absence of coherent weak interaction

§3.3 Inclusion of coherent weak interaction

§3.3.1 The adiabatic and the sudden regions

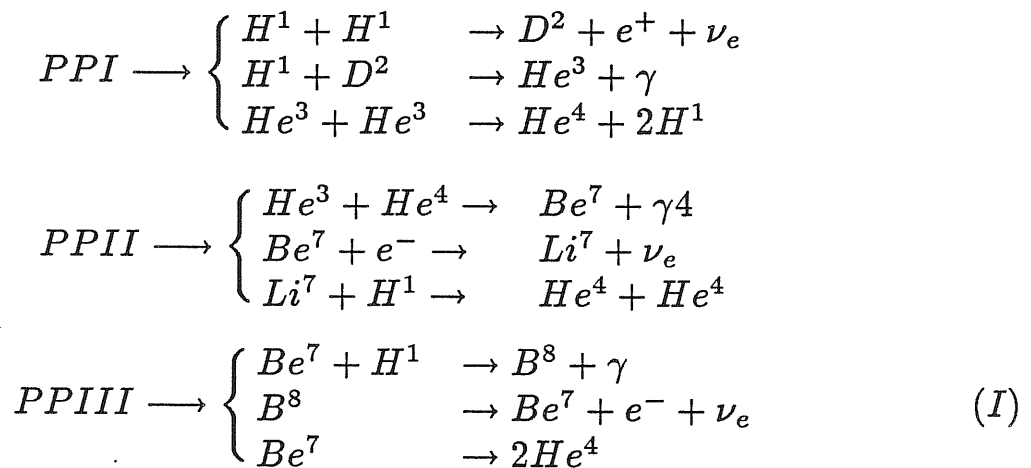
§3.3.2 The adiabatic and the sudden solutions

§3.3.3 Discussion

§3.4 Conclusions

INTRODUCTION

It is commonly accepted that stars, due to their long mean lifetime, are systems at hydrostatic equilibrium. Since stars continuously emit energy (in form of radiation or particles, with velocity higher than the escape velocity) this energy must be supplied to the star. The other key ingredients to describe the stellar evolution are nuclear combustions which provides energy and energy transport mechanism. If we limit our attention to stars being in an evolutive stage which is typical of the sun, the main contribution to the energy production is due to the so called PP chains



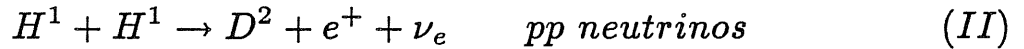
The relative importance of these different chains depends on the temperature in the core of the star.

Once that mechanisms for energy transport are known, the evolution equation for the state of the star can be determined. This equation links together the macroscopical variables of the system (luminosity, mass, temperature, pressure) and the microscopical mechanisms which determine them (energy transport and nuclear reaction).

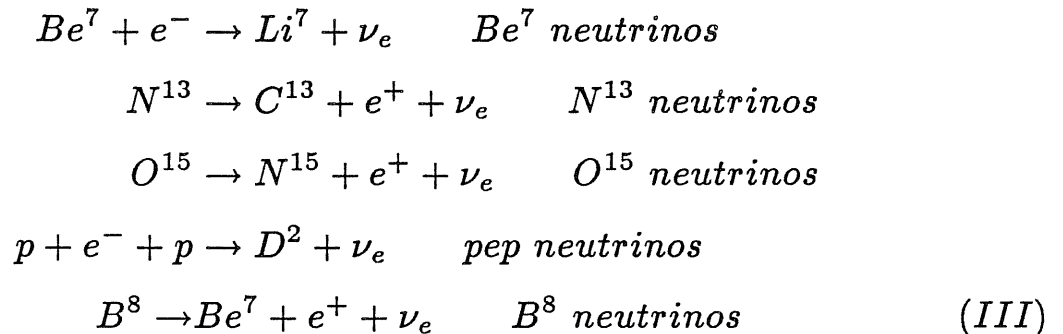
Given the state equation and the initial conditions (luminosity, mass, external temperature) it is possible to determine the complete state of the

system. In particular it is possible to determine the reaction rates for (I) and consequently the neutrino fluxes.

The main contribution to the solar neutrino flux is due to the reactions:



In addition there are the following reactions which are of much less importance for the energy balance:



In spite of the fact that reactions (III) are essentially negligible from the point of view of energy production, and the corresponding neutrino fluxes are much smaller in comparison with those due to reaction (II), Be^7 , pep , B^8 neutrinos are much easier to detect due to their higher energies.

At Homestake Davis and collaborators perform an experiment running since 1968 [1]. This experiment exploits the Cl-Ar radiochemical method for detection of solar neutrinos proposed by B. Pontecorvo. The method is based on the reactions



and is sensitive mainly to B^8 and Be^7 neutrinos. The expected capture rate for the experimental apparatus is 7.9 ± 2.6 SNU [2], (1 SNU is 10^{-36}

captures per target atom per second; the quoted error is claimed to be an effective 3σ error taking into account both theoretical uncertainty and uncertainty on the measured parameter which enters in the computation). More recently a competing group with a slightly different Standard Solar Model (SSM) gives an expectation of 5.8 ± 2.7 SNU [3].

The observed capture rate S_D [4] is

$$S_D = 2.33 \pm 0.25 \text{ SNU} \quad (V)$$

The discrepancy between the theoretical expectation and the experimental result constitutes the essence of the so called "Solar Neutrino Problem".

More recently (since 1986) another experiment has begun a systematic observation of the solar neutrinos. The Kamiokande II collaboration has developed a huge water Cherenkov detector which due to possibility to reconstruct the directions of the scattered positrons (with an accuracy of thirty degrees) is able to detect neutrinos from the sun above an energy of 7.5 Mev [5], observing the elastic scattering of neutrinos on the electrons.

The Kamiokande II experiment has two main differences with respect to the Davis one: it is sensible only to B^8 neutrinos, due to its threshold, and it is sensible also to ν_μ, ν_τ elastic scattering; this second aspect can play an important role in scenarios in which $\nu_e \rightarrow \nu_x$ ($\bar{\nu}_x$) conversion is postulated.

The Kamiokande II collaboration has confirmed the solar neutrino deficit observing [6] a fraction R_K of neutrinos with respect to the expected one from the SSM (Bahcall computation).

$$R_K = 0.46 \pm 0.05 \pm 0.06 \quad (VI)$$

Kamiokande II and Chlorine data not only disagree with the SSM but seem to be in disagreement between each other, the trend being that the Kamiokande II rate is larger than the Homestake one.

To have two (and possibly more) experiments is very important, since in principle the comparison between different experiments allows to eliminate uncertainty on the source which is intrinsic in this type of experiments.

More recently, a novel feature of the signal has been observed by the Homestake collaboration. It is claimed that the Homestake data are anti-correlated with the eleven years solar semicycle [7].

One way to see the correlation is to look for the signal at solar maxima and minima. Averaging over the two semicycles, during which homestake detector has taken data, the reported signal is [7]:

$$\begin{aligned} S_M^{(D)} &= 0.8 \pm 0.3 \text{ SNU} \\ S_m^{(D)} &= 4.1 \pm 0.6 \text{ SNU} \end{aligned} \tag{VII}$$

where $S_{M,m}^{(D)}$ is the signal detected at the maximum (minimum) of solar activity

The Kamiokande II collaboration claims to observe no such anticorrelation within a 30% accuracy [8].

It is very difficult to explain the solar neutrino deficit in terms of solar physics [9]. Since neutrino physics is the subject of this thesis, in the following we shall disregard this possibility and we will concentrate on neutrino physics, which possibly affects the solar neutrino signal.

We can group the properties of neutrinos, which have been suggested to solve the Solar Neutrino Problem, in three main classes:

- 1) Neutrino masses and mixing
- 2) Neutrino magnetic moment
- 3) Neutrino decay

We discuss only 1 and 2.

In the first chapter we discuss the hypothesis that neutrinos are massive and that the mass eigenstates do not coincide with the flavour eigenstates. If this is the case neutrino oscillations are expected: after a time t the initial ν_e can be converted into a ν_x , where ν_x can be both a usual flavour neutrino or a sterile one. This mechanism can explain the disappearance of a fraction of the emitted neutrinos.

The quantitative description of neutrino oscillation in the simplest case (two neutrino oscillations in vacuum) depends on three parameters: the vacuum mixing angle α , the difference of the squares of the different masses δm^2 , and the neutrino energy E . The probability P_{ex} of $\nu_e \rightarrow \nu_x$ conversion is an oscillating function of energy, however, for solar neutrinos with energy larger than 1 MeV, if $\delta m^2 \geq 10^{-10}$ eV the energy dependence either disappears, or it is averaged by the energy resolution of the detectors. Energy independent effects can account only for differences among detectors which are sensible only to ν_e and detectors which are sensible both to ν_e and to ν_x . The relevant region of parameters for the solution of the solar neutrino problem is

$$\frac{1}{3} \leq P_{ee} \leq 0.53 \quad \delta m^2 \geq 3 \times 10^{-10} \quad (VIII)$$

For a mass splitting δm of order $3 \times 10^{-10} \leq \delta m^2 \leq 3 \times 10^{-12}$ the probability to convert a ν_e into a ν_x is energy dependent. This range of δm can account for differences among detectors with different thresholds.

If we take into account that neutrinos inside the sun travel in a dense medium the previous scenario is modified. In the interior of the sun, neutrinos feel an effective potential, due to the coherent interaction of neutrinos with the stellar matter. Since the matter density varies inside the sun, the equation for the evolution of the neutrino states becomes an evolution equation with a potential which is time dependent. If the potential changes adiabatically during neutrino path from the interior to the surface of the sun, instantaneous eigenstates tend to remain instantaneous eigenstates and going out from the sun are converted to vacuum eigenstates. For some region of parameters a ν_e can be almost completely converted in a ν_x state.

Matter induced neutrino oscillations provide an energy dependent effect since both the adiabatic condition and the matter eigenstates depend on energy.

The relevant region of parameters is shown in fig. 2.

In the second chapter we discuss the hypothesis that neutrinos have unusual electromagnetic properties, such as an electric dipole moment or a magnetic moment. In this case, if the sun has a magnetic field which is coherent over large regions, some spin flip precession, due to the coherent interaction of neutrinos with the magnetic field of the sun, can occur. We observe a magnetic field at the solar surface whose intensity is correlated with the eleven years solar semicycle. This cycle is correlated to the activity in the convective zone and this probably implies that the magnetic field which is observed is confined inside the convective zone. The main interest in this effect is due to the fact that it can explain the claimed correlation of the signal with the solar activity.

The idea of spin flip was proposed by Cisneros [12] in connection with a possible magnetic field inside the inner core; this effect cannot explain the

time modulation of the signal. Later Okun, Visotsky and Voloshin revisited this idea and observed that if the spin flip is due to the magnetic field inside the convective zone some time modulation of the signal is expected. Their proposal was to consider a magnetic moment term connecting the left and right handed components of a Dirac neutrino. In this case only magnetic moment spin flip can occur and it is expected that in the periods of zero magnetic field the signal is the one predicted by the solar standard model. This does not seem in agreement with the data which show a deficit of order one half even at the maxima of solar activity. Additionally this hypothesis cannot account for a depletion as large as the observed one.

To resort this idea it has been proposed to consider both flavour oscillation and neutrino spin flip acting between two majorana neutrinos (both active, to avoid conflict with Supernova dynamics and primordial nucleosynthesis bounds on the number of neutrino species). These are the so called hybrid models.

Quantitative evaluations of the impact of these models on the solar neutrino signal are still lacunous but there are claims that for

$$\mu_\nu \simeq 10^{-11} \mu_B \quad B \simeq 20 \text{ kG} \quad (VII)$$

where μ_ν is the neutrino magnetic moment and B is the magnetic field in the solar interior, there is the possibility to reproduce the data.

At the end of the chapter we discuss an additional experimental signature of this class of models. Since we are concerned with majorana neutrinos no lepton number is conserved. This implies that some amount of $\bar{\nu}_e$ production is expected. For usual flavour neutrino oscillations this contribution is expected to be suppressed by a factor m_ν^2/E_ν^2 and thus negligible. In the case of Hybrid models the interplay of flavour oscillation which allows

$\nu_e \rightarrow \nu_x$ transitions and spin flip precession which allows $\nu_e \rightarrow \bar{\nu}_x$ transitions, can lead to a significant amount of $\bar{\nu}_e$ production.

It turns out that Kamiokande II experiment due to the large amount of almost free protons inside the detector is very sensitive to $\bar{\nu}_e$ through the reaction $\bar{\nu}_e + p \rightarrow n + e^+$. Looking at Kamiokande II data, we are able to limit the flux of $\bar{\nu}_e$ between 7.5 MeV and 15 MeV to be smaller than a fraction of order of few per cent of the emitted solar neutrinos.

$$\int de\Phi_{\bar{\nu}} \leq \Phi_{SSM} \quad (X)$$

where $\Phi_{\bar{\nu}}$ is the antineutrino flux and Φ_{SSM} is the solar neutrino flux according to the SSM.

This turns out to be enough to exclude all the classes of two neutrino hybrid models which require large mixing angle.

An additional potential problem for the theoretical implementation of this class of models is that they require two vastly different mass scales.

In the third chapter we propose an alternative hybrid model which overcomes both the difficulties we have outlined. We consider all the three neutrino flavours and we assume that the lepton number $L_e + L_\tau - L_\mu$ is conserved. The particle spectrum of this model consists of one massive Dirac neutrino and one massive Weyl neutrino. An unquenched spin flip can occur between the left and right helicity states of the Dirac neutrino while oscillation can occur between the Dirac neutrino and the Weyl one. The conservation law we assume overcomes both the problems we have outlined previously. The model we propose requires only one mass scale and does not predict $\bar{\nu}_e$ production.

Then we study the neutrino evolution problem postulating that the magnetic field is present only in the convective zone. We study only two limiting cases.

1) The magnetic field rises sharply at the beginning of the convective zone.

In this case almost any time modulation can be achieved. The required values for the input parameters are

$$\mu_\nu B \approx 10/R_\odot \quad (XI)$$

Since the probability is oscillating with the phase $\Phi = \int \mu B(r)$ we need $\Phi \simeq 1$

2) The magnetic field rises adiabatically at the beginning of the convective zone.

In this case the modulation cannot be larger than a factor two. The expression for the probability does not depend on the precise size of the magnetic field.

The required values for the input parameters are

$$\mu_\nu \geq 4/R_\odot \quad (XII)$$

The region of parameters for which we have adiabatic or sudden turning on is depicted in fig. 6

CHAP 1

NEUTRINO OSCILLATIONS IN VACUUM AND IN MATTER

In the following we consider the possibility that, due to some non standard physics, neutrinos can get a mass. Generally, in this case, neutrino flavour eigenstates do not coincide with mass eigenstates. Neutrinos emitted in weak interactions, therefore, are linear superpositions of wave packets of neutrinos with different masses. We now study the consequences of this assumption for the time evolution of a flavour neutrino state. This study is limited only to the possibility that neutrinos are Majorana particles and the number of massive neutrinos is just equal to the number of the observed neutrino flavours, namely to three.

§1.1 The Relevant Lagrangian for Neutrinos

For simplicity we limit the discussion to only two neutrinos since the extension to three neutrinos is straightforward.

In terms of the flavour neutrino fields, the kinetic term of the lagrangian density for neutrinos is

$$\begin{aligned} \mathcal{L} = & i\bar{\nu}_e(x)\gamma_\alpha\partial_\alpha\nu_e(x) + i\bar{\nu}_\mu(x)\gamma_\alpha\partial_\alpha\nu_\mu(x) \\ & + (m_{ee}\nu_e^T(x)C\nu_e(x) + m_{e\mu}\nu_e^T(x)C\nu_\mu(x) \\ & + m_{\mu e}\nu_\mu^T(x)C\nu_e(x) + m_{\mu\mu}\nu_\mu^T(x)C\nu_\mu(x) + h.c.) \end{aligned} \quad (1.1)$$

where C is the charge conjugation matrix.

Due to the relation $C = -C^T$ and to the anticommutation of the spinor fields we get $m_{e\mu} = m_{\mu e}$.

The complex phases of m_{ee} and $m_{\mu\mu}$ can be reabsorbed redefining the phases of ν_e and ν_μ and these phases can be eliminated from the lagrangian using the freedom of redefining the phases of the electron and muon fields which are unobservable. So at the end we are left with only one physically relevant phase[13].

Taking m_{ee} and $m_{\mu\mu}$ real and $m_{e\mu} = me^{i\delta}$, we define the Majorana neutrino fields ν_1, ν_2 as:

$$\begin{aligned}\nu_1 &= \cos \alpha \nu_e - e^{-i\delta} \sin \alpha \nu_\mu \\ \nu_2 &= e^{i\delta} \sin \alpha \nu_e + \cos \alpha \nu_\mu\end{aligned}\tag{1.2}$$

where

$$\tan 2\alpha = \frac{2m}{m_{ee} - m_{\mu\mu}}\tag{1.3}$$

The Lagrangian (1.1) can be rewritten as:

$$\begin{aligned}\mathcal{L} &= i\bar{\nu}_1(x)\gamma_\alpha\partial_\alpha\nu_1(x) + i\bar{\nu}_2(x)\gamma_\alpha\partial_\alpha\nu_2(x) \\ &+ m_1\nu_1^T(x)C\nu_1(x) + m_2\nu_2^T(x)C\nu_2(x)\end{aligned}\tag{1.4}$$

where

$$\begin{aligned}m_1 &= \frac{1}{2}(m_{ee} + m_{\mu\mu} + \sqrt{(m_{ee} - m_{\mu\mu})^2 + 4m^2}) \\ m_2 &= \frac{1}{2}(m_{ee} + m_{\mu\mu} - \sqrt{(m_{ee} - m_{\mu\mu})^2 + 4m^2})\end{aligned}\tag{1.5}$$

§1.2 Propagation of a flavour neutrino state in vacuum

We now study the propagation in the vacuum of an electron neutrino produced in some weak process. If this neutrino has been created at the point \mathbf{x}_0 and time $t_0 = 0$, the neutrino wave packet is:

$$|\psi_e(\mathbf{x})\rangle = \int d\mathbf{p} [a(\mathbf{p}) |\nu_{1\mathbf{p}}\rangle e^{i\mathbf{p}(\mathbf{x}-\mathbf{x}_0)} + b(\mathbf{p}) |\nu_{2\mathbf{p}}\rangle e^{i\mathbf{p}(\mathbf{x}-\mathbf{x}_0)}] \quad (1.6)$$

where $a(\mathbf{p})$ and $b(\mathbf{p})$ are momentum distribution peaked around the momenta \mathbf{p}_1 and \mathbf{p}_2 respectively and with width Δp_1 and Δp_2 . In the relativistic limit $\mathbf{p}_1 \simeq \mathbf{p}_2 = \mathbf{p}_0$, $a(\mathbf{p}) \simeq \cos \alpha a_0(\mathbf{p})$ and $b(\mathbf{p}) \simeq \sin \alpha a_0(\mathbf{p})$

After a time t the neutrino propagates in the following way

$$|\psi_e(\mathbf{x}, t)\rangle = \int d\mathbf{p} [a(\mathbf{p}) |\nu_{1\mathbf{p}}\rangle e^{i(\mathbf{p}(\mathbf{x}-\mathbf{x}_0) - E_1 t)} + b(\mathbf{p}) |\nu_{2\mathbf{p}}\rangle e^{i(\mathbf{p}(\mathbf{x}-\mathbf{x}_0) - E_2 t)}] \quad (1.7)$$

where $E_j(\mathbf{p}) = \sqrt{p^2 + m_j^2}$

Therefore at time t the wave packet will be located around a point \mathbf{x}_1 at a distance $d = vt$, v denoting the velocity of the neutrino wave packet. For a relativistic neutrino $v = c$ and so $\mathbf{p}(\mathbf{x}_0 - \mathbf{x}_1) \simeq pt$.

Now we want to investigate the probability for the emitted neutrino to be detected at a time t as an electron neutrino located around \mathbf{x}_1 . If the neutrino wave packets spatially overlap we must add the amplitudes, otherwise we must add probabilities.

If we assume the two neutrino wave packets overlap, using (1.6) and (1.7) we get: $\mathcal{A}_{ee} = \langle \psi_e(\mathbf{x}_1) | \psi_e(\mathbf{x}_0, t) \rangle$

$$\mathcal{A}_{ee} = \int d\mathbf{p} [\cos \alpha a_0(\mathbf{p}) e^{i(\mathbf{p}(\mathbf{x}_1 - \mathbf{x}_0) - E_1 t)} + \sin \alpha a_0(\mathbf{p}) e^{i(\mathbf{p}(\mathbf{x}_1 - \mathbf{x}_0) - E_2 t)}] \quad (1.8)$$

For small $\Delta p/p$ and m/p we get $m_j^2/2p = m_j^2/2p_0$ and $E_j(\mathbf{p}) = p + m_j^2/2p$. In this limit we get from (1.8)

$$\mathcal{A}_{ee} = \int d\mathbf{p} [\cos \alpha a_0(\mathbf{p}) e^{-im_1^2 t/2p} + \sin \alpha a_0(\mathbf{p}) e^{-im_2^2 t/2p}] \quad (1.9)$$

Exactly in the same way taking for the ν_μ state the orthogonal one to ν_e state we get $\mathcal{A}_{e\mu}$. Taking the square of the probability amplitude we get the probability P_{ex} to detect the original ν_e as a ν_x

$$\begin{aligned} P_{ee}(t) &= 1 - \frac{1}{2} \sin^2 2\alpha (1 - \cos \Phi) \\ P_{e\mu}(t) &= \frac{1}{2} \sin^2 2\alpha (1 - \cos \Phi) \\ \Phi &= \frac{m_2^2 - m_1^2}{2p} t \end{aligned} \quad (1.10)$$

The mechanism we have described is known as neutrino oscillation [11].

As we have already outlined, for relativistic neutrinos time and distance are equivalent and in the previous equation we can substitute t with R where R is the distance between the points \mathbf{x}_0 and \mathbf{x}_1 . After this substitution we can define an oscillation length $L_0 = 4\pi E/(m_1^2 - m_2^2)$ which is the distance after which the phase Φ takes the value 2π .

Since it is an interference phenomenon it can occur only if the two neutrino wave packets overlap spatially. Due to different masses the two neutrino wave packets experience different velocities and after a time $t = t_d$ will no more overlap and the interference phenomenon will disappear.

The relative velocity v_{rel} between the two neutrino wave packets is

$$v_{rel} = \frac{p}{\epsilon_2} - \frac{p}{\epsilon_1} \simeq -\frac{p}{p^2} \left(\frac{m_2^2}{2p} - \frac{m_1^2}{2p} \right) = \frac{m_1^2 - m_2^2}{2p^2} \quad (1.11)$$

From (1.11) follows that the mean spatial separation $\langle D(t) \rangle$ between the two neutrino wave packets is

$$\langle D(t) \rangle = \frac{m_1^2 - m_2^2}{2p^2} t \quad (1.12)$$

If the typical spatial spread of the initial packet is δx the two neutrino no more overlap when $\langle D(t) \rangle \geq \delta x$ which can be translated on a condition over the time. If we define the decoupling time t_d as

$$\begin{aligned} \delta x &= \langle D(t_d) \rangle \\ t_d &= \frac{2p^2}{m_1^2 - m_2^2} \delta x \end{aligned} \quad (1.13)$$

If $t > t_d$ holds, no interference occurs between ν_1, ν_2 and we can no more add the amplitudes for ν_1 and ν_2 to be ν_e or ν_μ . We must add probabilities. In this case we get

$$\begin{aligned} P_{ee} &= 1 - \frac{1}{2} \sin^2 2\alpha \\ P_{e\mu} &= \frac{1}{2} \sin^2 2\alpha \end{aligned} \quad (1.14)$$

which doesn't show any time or energy dependence.

§1.3 Relevance of Vacuum Neutrino Oscillation for the Solar Neutrino Problem

We shall now assume that vacuum neutrino oscillations occur between the sun and the earth and we shall examine briefly their implication for the solar neutrino signal which is detected by solar neutrino experiments.

The signal S_D in the Chlorine experiment is

$$S_D = TN\epsilon \int_{E_{th}}^{E_{end}} dE \Phi(E) \sigma(E) P_{ee}(E) \quad (1.15)$$

where $\Phi(E)$ is the differential flux of solar neutrinos, $\sigma(E)$ is the absorption cross section for the reaction $\nu_e + Cl^{37} \rightarrow e^- + Ar^{37}$, E_{th} is the threshold energy for the detection of the signal, E_{end} is the end point energy of the spectrum, T is the detection time, N is the number of scatterers and ϵ is the efficiency for the extraction of Ar^{37} from the detector.

The signal S_K in Kamioka experiment is

$$S_K = TN \int_{E_{th}}^{E_{end}} dE \Phi(E) \epsilon(E) [(\sigma_e(E) P_{ee}(E) + \sigma_\mu(E) P_{e\mu}(E))] \quad (1.16)$$

where σ_x is the elastic cross section for $\nu_x e$ scattering

Now it arise the question of weather we have to take into account energy dependence of the probability as in (1.10) or we can average the oscillating term as in (1.14) obtaining an energy independent probability.

We define $\Delta = m_1^2 - m_2^2$. There are three points to take into account

a) the condition for spatial overlapping of the two wave packets. This problem has been investigated by Nussinov [14] and it turns out that spatial overlap requires:

$$\frac{\Delta}{E_\nu^2} \leq 10^{-21} \quad (1.17)$$

b) If the oscillation length is not larger than the sun inner core averaging over the region of production of the neutrinos is equivalent to average over the oscillating term which gives one half contribution[15]. If

$$\frac{E_\nu}{\Delta} \geq 10^{-2} R_\odot \quad (1.18)$$

where R_\odot is the solar radius, than vacuum oscillation length is larger than the production zone.

c) If the product $R_{se}(m_1^2 - m_2^2)/4$, where R_{se} is much larger than the typical energy of neutrinos which are detected the contribution of the oscillating term is again averaged to one half, due to the finite energy resolution of the detectors [15]. If

$$3 \times 10^{-10} \leq \Delta \leq 3 \times 10^{-12} \text{eV}^2 \quad (1.19)$$

than the detector energy resolution does not average the oscillating term.

Unless (1.17 ÷ 1.19) are satisfied the oscillating term is unobservable and no energy dependent effect can arise. Additionally oscillation turns out to be ineffective for oscillation length which are larger than the sun earth distance since in this case $P_{ee} = 1$ and $P_{\mu\mu} = 0$.

The region of parameters for which the probabilities are energy dependent has been investigated in [15]. For:

$$5 \times 10^{-10} \leq \Delta \leq 1.1 \times 10^{-11} \quad \sin^2 2\alpha \geq 0.7 \quad (1.20)$$

it is possible to reconcile within the experimental errors the two signals.

If the oscillating term can be averaged the probability can be taken out of the integral. If we assume that neutrino oscillates only in active neutrino we get (see (1.15) and (1.16))

$$\begin{aligned} R_D &= \beta_D P_{ee} \\ R_K &= \beta_K [P_{ee} + (1 - P_{ee}) \bar{\sigma}_\mu / \bar{\sigma}_e] \\ \bar{\sigma}_x &= \int_{E_{th}}^{E_{end}} dE \Phi(E) \sigma_x(E) \end{aligned} \quad (1.21)$$

where R_D and R_K are the ratios of the detected signals and the central value of the theoretical expectation, $\beta_D = 1 \pm 0.33$ and $\beta_K = 1 \pm 0.37$

are two factors which take into account the theoretical uncertainties or the neutrino fluxes, for Davis and Kamioka experiment respectively.

Taking into account possible oscillations between all the three neutrino flavours it must be $P_{ee} \geq 1/3$ (if a neutrino is a linear superposition of n neutrino mass eigenstates, $\nu_e = \sum_{i=1}^n a_i \nu_i$, averaging the oscillating terms in the probabilities we get $P_{ee} = \sum_{i=1}^n |a_i|^4$ and for the three neutrino system the minimum value for P_{ee} is $1/3$). Having in mind this restriction to reconcile the two signals require

$$\frac{1}{3} \leq P_{ee} \leq 0.53 \quad \Delta > 3 \times 10^{-10} (\text{eV})^2 \quad (1.22)$$

where we have considered 2σ intervals for both experiments and we have allowed a 3σ deviation from the central value of the theoretical expectation.

§1.4 Matter neutrino oscillation

The neutrinos we are considering are born in the sun and for a time of about two seconds travel inside the sun which is a relatively dense medium. Matter density is not enough to provide significant cross section for neutrino scattering, however we shall see that under certain conditions it can greatly modify the neutrino wave packet evolution.

§1.4.1 The propagation of a neutrino in a dense medium

The neutrino travelling in the medium is a coherent superposition of states $|\nu_{j\text{p}}\rangle$ as in (1.6), whereas the medium is a completely incoherent sum of different fermionic states $|f_{\text{q}}\rangle$.

We now want to understand the time evolution of the system.

The amplitude $A_{\psi\psi'}$ for a state ψ at a time t_0 to become a state ψ' at a time $t_0 + \Delta t$ is:

$$A_{\psi\psi'} = \langle \psi' | T \exp\left(i \int_{t_0}^{t_0 + \Delta t} dt L_{int}\right) | \psi \rangle$$

$$L_{int} = \int_{R^3} d\mathbf{x} \mathcal{L}_{int} \quad (1.23)$$

where \mathcal{L}_{int} is the interacting sector of the lagrangian density.

Since we want to compute the time evolution we need to consider the small Δt limit. Essentially we need Δt much less than the typical mean free path of neutrinos. On the other hand for (1.23) to be of any use (read calculable) Δt must be much larger than the typical collision time in order we can apply asymptotic states limit in the computation of the S matrix. In the case under consideration the typical mean free path is much larger than the sun and we can safely compute (1.23) with the ordinary methods.

Since scattering and absorption effects are negligible $A_{\psi\psi'}$ can be relevant only if $|\psi'\rangle$ coherently superimpose to the unscattered state $|\psi\rangle$ giving rise to interference effects. Let's now discuss the condition for which this happens.

Since neutrino state is a coherent superposition of two neutrino wave packets ν_1 and ν_2 we can allow for

a) $|\nu_1\rangle \rightarrow |\nu_2\rangle$ transition

b) Small momentum changes $\Delta \mathbf{p} < \delta \mathbf{p}$ where $\delta \mathbf{p}$ is the typical momentum spread of the wave packet

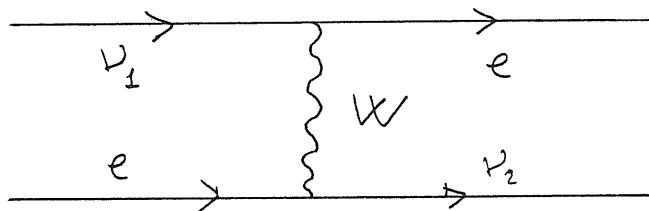
For the medium since it is an incoherent superposition of states we must require that the initial and final states are equal.

The condition for the medium implies that only forward scattering amplitude is relevant, neutrino initial and final momenta must be the same.

§1.4.2 Forward scattering amplitudes

Spinors and field we use to compute (1.23) are described in appendix A.

The medium is constituted of ordinary matter and we will need to consider the elastic scattering off electrons, protons and neutrons. We shall now consider in detail the amplitude \mathcal{A} for the process



$$\nu_{1\mathbf{p}}^L + e_{\mathbf{q}} \rightarrow \nu_{2\mathbf{p}}^L + e_{\mathbf{q}} \quad (1.24)$$

where with $\nu_j^{(L,R)}$ we denote ν_j neutrinos with left (right) handed polarization. From (1.23) and we get:

$$\begin{aligned} \mathcal{A} = & \langle 0 | a_{\nu_{2\mathbf{p}}}^L a_{e\mathbf{q}} [T i \int_{t_0}^{t_0+\Delta t} \int d\mathbf{x} \frac{G}{\sqrt{2}} \sin \alpha \cos \alpha e^{i\delta} e^{-i(p_{01}-p_{02})t_0} \\ & \times \bar{\nu}_2(x) \gamma_\mu (1 + \gamma_5) e(x) \bar{e}(x) \gamma_\mu (1 + \gamma_5) \nu_1(x) + \dots + h. c.] a_{e\mathbf{q}}^\dagger a_{\nu_{1\mathbf{p}}}^L | 0 \rangle \end{aligned} \quad (1.25)$$

where $a_{x\mathbf{p}}^\dagger$ is the creation operator for a particle x with momentum \mathbf{p} , and the factor $e^{-i(p_{01}-p_{02})t_0}$ takes into account that we are working in the interaction picture.

Normalizing properly at a density of one neutrino per unit volume and N_e electron per unit volume we get:

$$\begin{aligned}
\mathcal{A} &= -i \frac{G}{\sqrt{2}} \frac{\cos \alpha \sin \alpha N_e}{4q_0 \sqrt{p_{01} p_{02}}} \bar{e}(\mathbf{q}) \gamma_\mu (1 + \gamma_5) e(\mathbf{q}) \int_{t_0}^{t_0 + \Delta t} dt e^{i(p_{02} - p_{01})t_0} \\
&\times [e^{i\delta} \bar{\nu}_2(\mathbf{p}) \gamma_\mu (1 + \gamma_5) \nu_1(\mathbf{p}) + \nu_1^T(\mathbf{p}) C \gamma_\mu (1 + \gamma_5) C \nu_2^*(\mathbf{p}) e^{-i\delta}] \\
&= -i \Delta t \frac{G \cos \alpha \sin \alpha N_e}{4q_0 \sqrt{p_{01} p_{02}}} \bar{e} \gamma_\mu (1 + \gamma_5) e \\
&\times [\bar{\nu}_2 \gamma_\mu (1 + \gamma_5) \nu_1 e^{i\delta} + \nu_1^T C \gamma_\mu (1 + \gamma_5) C \nu_2^*] + O(\Delta^2 t) \quad (1.26)
\end{aligned}$$

For the evolution equation we need $\mathcal{V} = i \frac{\Delta}{\Delta t} \mathcal{A}$. Averaging over the electron spin we get:

$$\begin{aligned}
\mathcal{V}_{1,2}^L &= i \frac{\Delta}{\Delta t} \mathcal{A} = \frac{G \cos \alpha \sin \alpha N_e}{\sqrt{2} 2q_0 \sqrt{p_{01} p_{02}}} \\
&\times q_\mu [\bar{\nu}_2 \gamma_\mu (1 + \gamma_5) \nu_1 e^{i\delta} + \nu_1^T C \gamma_\mu (1 + \gamma_5) C \nu_2^* e^{-i\delta}] \quad (1.27)
\end{aligned}$$

in the rest frame of the medium $\langle \mathbf{q} \rangle = 0$ and finally we get:

$$\begin{aligned}
\mathcal{V}_{1,2}^L &= \frac{GN_e \cos \alpha \sin \alpha}{\sqrt{2} \sqrt{(p_{01} + m_1)(p_{02} + m_2)p_{01} p_{02}}} \{ 2[(p_{01} + m_1)(p_{02} + m_2) + p^2] \cos \delta + \\
&+ 2ip(p_{01} + p_{02} + m_1 + m_2) \sin \delta \} \quad (1.28)
\end{aligned}$$

In the same way we get the other contributions

$$(1.29)$$

It follows

$$\begin{aligned}\mathcal{V}_{1,1}^L &= \frac{G}{\sqrt{2}} \frac{p}{p_{01}} (2N_e \cos^2 \alpha - GN_n) \\ \mathcal{V}_{2,2}^L &= \frac{G}{\sqrt{2}} \frac{p}{p_{01}} (2N_e \sin^2 \alpha - GN_n)\end{aligned}\quad (1.30)$$

Transition $|\nu_{1,2p}^L\rangle |e_q^{(\alpha)}\rangle \rightarrow |\nu_{1,2p}^R\rangle |e_q^{(\alpha)}\rangle$ are forbidden by angular momentum conservation and this can be verified explicitly, so we get

$$\mathcal{V}_{1,1}^{L,R} = \mathcal{V}_{1,2}^{L,R} = \mathcal{V}_{2,1}^{L,R} = \mathcal{V}_{2,2}^{L,R} = 0 \quad (1.31)$$

for transition of right handed polarized states we get in general $\mathcal{V}^L = -\mathcal{V}^{R*}$

$$\begin{aligned}\mathcal{V}_{1,1}^R &= -\frac{G}{\sqrt{2}} \frac{p}{p_{01}} (2N_e \cos^2 \alpha - GN_n) \\ \mathcal{V}_{2,2}^R &= -\frac{G}{\sqrt{2}} \frac{p}{p_{01}} (2N_e \sin^2 \alpha - GN_n)\end{aligned}$$

$$\begin{aligned}\mathcal{V}_{1,2}^R &= -\frac{GN_e \cos \alpha \sin \alpha}{\sqrt{2} \sqrt{(p_{01} + m_1)(p_{02} + m_2)p_{01}p_{02}}} \{2[(p_{01} + m_1)(p_{02} + m_2) + p^2] \cos \delta + \\ &\quad - 2ip(p_{01} + p_{02} + m_1 + m_2) \sin \delta\}\end{aligned}\quad (1.32)$$

§1.4.3 Neutrino evolution equation in matter

If the neutrino state at a time t is

$$|\nu^{L,R}(t)\rangle = d_1^{L,R}(t) |\nu_1\rangle^{L,R} + d_2^{L,R}(t) |\nu_2\rangle^{L,R} \quad (1.33)$$

the evolution equation in matter is

$$i \frac{\partial}{\partial t} d_j^{L,R} = H_{j,k}^{L,R} d_k^{L,R} \quad (1.34)$$

where

$$\begin{aligned}
H^L &= \begin{pmatrix} E_1 + \mathcal{V}_{1,1}^L & \mathcal{V}_{1,2}^L \\ \mathcal{V}_{1,2}^{L*} & E_2 + \mathcal{V}_{2,2}^L \end{pmatrix} \\
H^R &= \begin{pmatrix} E_1 + \mathcal{V}_{1,1}^R & \mathcal{V}_{1,2}^R \\ \mathcal{V}_{1,2}^{R*} & E_2 + \mathcal{V}_{2,2}^R \end{pmatrix}
\end{aligned} \tag{1.35}$$

The importance of this equation in analyzing neutrino oscillation in matter was pointed out by Wolfenstein[16].

We define

$$\begin{aligned}
E^\pm &= (E_1 + E_2 + \mathcal{V}_{1,1}^L + \mathcal{V}_{2,2}^L)/2 \\
\epsilon &= (E_1 - E_2 + \mathcal{V}_{1,1}^L - \mathcal{V}_{2,2}^L)/2 \\
\delta^\pm &= \mathcal{V}_{1,2}^{L,R}
\end{aligned} \tag{1.36}$$

The Hamiltonian is

$$H^\pm = \begin{pmatrix} E^\pm & 0 \\ 0 & E^\pm \end{pmatrix} + \begin{pmatrix} \epsilon^\pm & \delta^\pm \\ \delta^{\pm*} & -\epsilon^\pm \end{pmatrix} \tag{1.37}$$

The diagonal term can be reabsorbed in a redefinition of the amplitude $a_j(t)$. With

$$\begin{aligned}
A_j(t) &= e^{-iEt} a_j(t) \\
\mathcal{H} &= \begin{pmatrix} \epsilon & \delta \\ \delta^* & -\epsilon \end{pmatrix}
\end{aligned} \tag{1.38}$$

we get

$$i \frac{\partial}{\partial t} A_j(t) = \mathcal{H}_{jk} A_k(t) \tag{1.39}$$

If $\delta = \delta_0 e^{i\delta_1}$ using the unitary transformation

$$U_m = \begin{pmatrix} \cos \alpha_m & -\sin \alpha_m e^{i\delta_1} \\ \sin \alpha_m e^{-i\delta_1} & \cos \alpha_m \end{pmatrix}$$

$$\tan 2\alpha_m = \frac{\delta}{\epsilon} \quad (1.40)$$

we can diagonalize \mathcal{H}

$$\mathcal{H}_D = U_m \mathcal{H} U_m^\dagger$$

$$\mathcal{H}_D = \begin{pmatrix} \sqrt{\epsilon_0^2 + \delta_0^2} & 0 \\ 0 & -\sqrt{\epsilon_0^2 + \delta_0^2} \end{pmatrix} \quad (1.41)$$

If \mathcal{V} is constant in time following (1.41) the evolution problem is solved.

Solar neutrinos, of interest for the experiment we are discussing, for masses below 1 MeV are relativistic. Since we are interested to discuss the effect of matter induced oscillation for solar neutrinos we give the relativistic limit for the previous equations. We choose, for convenience, to give the expression in the flavour basis.

$$\mathcal{H}_{(r)}^L = \begin{pmatrix} \cos 2\alpha \frac{\Delta}{4E} + \mathcal{V}_e & \sin 2\alpha e^{-i\delta} \frac{\Delta}{4E} \\ \sin 2\alpha e^{i\delta} \frac{\Delta}{4E} & -\cos 2\alpha \frac{\Delta}{4E} + \mathcal{V}_\mu \end{pmatrix}$$

$$\mathcal{H}_{(r)}^R = \begin{pmatrix} \cos 2\alpha \frac{\Delta}{4E} - \mathcal{V}_e & \sin 2\alpha e^{-i\delta} \frac{\Delta}{4E} \\ \sin 2\alpha e^{i\delta} \frac{\Delta}{4E} & -\cos 2\alpha \frac{\Delta}{4E} - \mathcal{V}_\mu \end{pmatrix} \quad (1.42)$$

where

$$\mathcal{V}_e = G\sqrt{2}n_e - \frac{G}{\sqrt{2}}n_n$$

$$\mathcal{V}_\mu = -\frac{G}{\sqrt{2}}n_n \quad (1.43)$$

The matrix $\mathcal{H}_{(r)}$ is diagonalized by the transformation

$$\mathcal{H}_D = U_m \mathcal{H} U_m^\dagger$$

$$U_m = \begin{pmatrix} \cos \alpha_m & -\sin \alpha_m e^{i\delta_1} \\ \sin \alpha_m e^{-i\delta_1} & \cos \alpha_m \end{pmatrix}$$

$$\tan 2\alpha_m = \frac{\sin 2\alpha \frac{\Delta}{4E}}{\cos 2\alpha \frac{\Delta}{4E} + \frac{G}{\sqrt{2}} n_e} \quad (1.44)$$

$$\mathcal{H}_D = \begin{pmatrix} -\bar{\lambda} & 0 \\ 0 & \bar{\lambda} \end{pmatrix} \quad (1.45)$$

$$\bar{\lambda} = \sqrt{\left(\cos 2\alpha \frac{\Delta}{4E} + \frac{G}{\sqrt{2}} n_e\right)^2 + \left(\sin 2\alpha \frac{\Delta}{4E}\right)^2} \quad (1.46)$$

§1.4.4 The M. S. W. effect

However in the sun the density is not constant and in its travel neutrino experience different densities and so a potential \mathcal{V} which is not constant in time. Neutrinos are relativistic and $R = t$ if R is the distance between the point in which the neutrino is emitted and the point it reaches at the time t . Equation (1.39) becomes

$$i \frac{\partial}{\partial R} A = \mathcal{H}_{(r)}(R) A \quad (1.47)$$

Where the R dependence of $\mathcal{H}_{(r)}$ is completely described by the R dependence of electron and neutron densities $N_e(R)$, $N_n(R)$.

Using the diagonalization (1.41)-(1.42) and taking into account that α_m is a function of R we get

$$i \frac{\partial}{\partial R} \begin{pmatrix} B_1 \\ B_2 \end{pmatrix} = \begin{pmatrix} \lambda(R) & 0 \\ 0 & -\lambda(R) \end{pmatrix} \begin{pmatrix} B_1 \\ B_2 \end{pmatrix} + \begin{pmatrix} 0 & i \frac{\partial \alpha_m}{\partial R} \\ -i \frac{\partial \alpha_m}{\partial R} & 0 \end{pmatrix} \begin{pmatrix} B_1 \\ B_2 \end{pmatrix} \quad (1.48)$$

where $B_j = U_{m \ j k} A_k$.

In general equation (1.48) is not exactly solvable. However two important limits are easily under control.

$$\alpha_m(R) \gg \lambda(R) \tag{1.49}$$

this corresponds to the impulsive limit, the time variation is too fast and the state doesn't change.

$$\alpha_m(R) \ll \lambda(R) \tag{1.50}$$

this corresponds to the adiabatic regime. In the limit in which α_m is negligible we get for the evolution of a state $|\nu_{j,t=0}\rangle$ which at a time t is an eigenvector of \mathcal{H} with eigenvalue λ_j

$$|\nu_{j,t=0}(t)\rangle \rightarrow |\nu_{j,t}\rangle \exp -i \int_0^t ds \lambda_j(s) \tag{1.51}$$

where $|\nu_{j,t}\rangle$ are the instantaneous eigenstates of the hamiltonian $\mathcal{H}(t)$ at the time t .

$|\nu_{j,t}\rangle$ evolves staying an instantaneous eigenstate $|\nu_{j,t}\rangle$ of the Hamiltonian.

§1.4.5 Relevance of neutrino mixing in matter for the solar neutrino problem

If impulsive condition (1.49) holds the neutrino state is lefted unchanged and the evolution is the same as in vacuum. Conversely if adiabatic condition holds the picture is drastically altered. As we have already stressed, for relativistic neutrinos time and distance are completely equivalent and we can substitute the time t with the position R in the equation for the evolution of the neutrino.

If ν_{jm} are the instantaneous eigenstates in matter, the initial neutrino state, at the point R_i in the interior of the sun, is:

$$|\nu_e(R_i)\rangle = \cos \alpha_m(R_i) |\nu_{1m}\rangle + \sin \alpha_m(R_i) |\nu_{2m}\rangle \quad (1.52)$$

In a point R_f at the surface of the sun, the ν_e states becomes

$$\nu_e(R_f) = \cos \alpha_m(R_i) |\nu_1\rangle + \sin \alpha_m(R_i) |\nu_2\rangle \quad (1.53)$$

Projecting the neutrino states $\nu_e(R_i)$ over the ν_e state in vacuum, we get the amplitude \mathcal{A}_{ee} for the emitted ν_e to emerge outside the sun as ν_x

$$\mathcal{A}_{ee} = \cos \alpha_m(R_i) \cos \alpha e^{-i \int_{R_i}^{R_f} ds \lambda_j(s)} + \sin \alpha_m(R_i) \sin \alpha e^{i \int_{R_i}^{R_f} ds \lambda_j(s)} \quad (1.54)$$

For the outcoming probability we get

$$P_{ee} = \cos^2 \alpha_m(R_i) \cos^2 \alpha + \sin^2 \alpha_m(R_i) \sin^2 \alpha + 2 \sin \alpha_m(R_i) \sin \alpha \cos \alpha_m(R_i) \cos \alpha \cos \int_{R_i}^{R_f} ds \lambda_j(s) \quad (1.55)$$

This relation was found by Micaiev and Smirnov [17]. Particularly simple is the small α limit: $\cos \alpha = 1$ and $\sin \alpha = O(\alpha)$. In this case we get, neglecting $O(\alpha)$ terms:

$$P_{ee} = \cos^2 \alpha_m(R_i) \cos^2 \alpha \quad (1.56)$$

where, if $\Delta < 0$,

$$\cos^2 \alpha_m(R_i) = \frac{1}{2} \left(1 - \frac{\frac{\Delta \cos 2\alpha}{4E} + \frac{Gn_e}{\sqrt{2}}}{\sqrt{\frac{\Delta^2}{16E^2} + \sqrt{2}Gn_e \cos 2\alpha \frac{\Delta}{4E} + \frac{G^2 n_e^2}{2}}} \right) \quad (1.57)$$

If $\Delta < 0$ and $\Delta \cos 2\alpha/4E + Gn_e(R_i)/\sqrt{2} > 0$, $\cos^2 \alpha_m(R_i)$ is a decreasing function of energy.

Both the probability (1.56) and the adiabatic condition are energy dependent and so the MSW effect is energy dependent. The adiabatic condition is better satisfied with decreasing energy, while the probability (1.56), at least for small mixing angle decreases with energy. According to the choice of parameters it is possible to account for a larger depletion of both the higher energy neutrinos and the lower energy one. To make more quantitative comparisons with experiments an analytic interpolation between impulsive and adiabatic condition is needed. In particular equation (1.39) can be solved exactly for $N_e(R) = N_0 + N_1 R$ [18] and for $N_e(R) = N_0 \exp(-kR)$ [19]. The second one is a good representation of the solar density profile, while the first one has to be used as an expansion for $N_e(R)$ around the resonant point. This work has been done by many people (see [20] for example). The region of parameters consistent with the experimental data (however without taking into account theoretical uncertainty) is shown in fig1

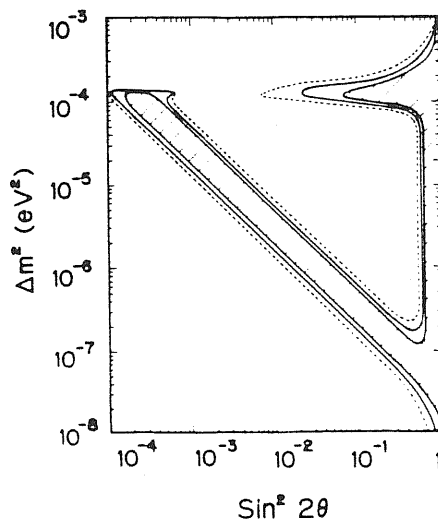


FIG. 1. The confidence level contours at the 68 % (hatched) 90 % (solid line), and 95 % (dashed line) for the "allowed"

regions of the MSW solutions which were obtained from both the total flux measured by KAM II and Homestake and the measured recoil electron energy spectrum.

In conclusion matter induced neutrino oscillation have the following feature:

- a) they can provide significant depletion of the neutrino signal with $\sin^2 2\alpha \geq 10^{-4}$
- b) Their effect is energy dependent.

CHAPTER 2

NEUTRINO SPIN PRECESSION IN A COHERENT MAGNETIC FIELD

Observational data show the existence of a magnetic field at the surface of the sun. The magnitude of this field is strongly correlated with solar activity, the twentytwo years solar cycle. This correlation implies that this field is connected with the solar activity in the convective region of the sun. Additionally it has been postulated (without any experimental evidence), that a inner magnetic field can be present inside the most interior region of the sun, the "quiet" sun. This inner field, if it exists, cannot be correlated with solar activity. If we postulate the existence of unconventional neutrino magnetic properties, such as a neutrino magnetic moment, some coherent effect of the same kind we have described in the previous chapter can occur [20]. Additionally if this effect is connected with the field of the convective region some correlation with the solar activity is expected [20]. This feature reproduces the claimed correlation of the Chlorine data with solar activity and motivates the large interest in this effect.

§2.1 Effective Lagrangian Accounting for Neutrino Electromagnetic Properties

Since neutrinos are electrically neutral, the most effective coupling (at low q^2 where q is the four momentum carried by the photon) of neutrinos to

photons is of electric and magnetic dipole moment type. We are therefore induced to look for effective couplings of the type

$$\mathcal{L}_{em} = \mu_{jk} \bar{\chi}_j \sigma_{\alpha\beta} \chi_k F_{\alpha\beta} + i d_{jk} \bar{\chi}_j \sigma_{\alpha\beta} \gamma_5 \chi_k F_{\alpha\beta} \quad (2.1)$$

μ_{jk} and d_{jk} are the magnetic and electric dipole moment respectively, χ_j and χ_k are the Majorana field of ν_j and ν_k neutrinos with $\chi_j = C \bar{\chi}_j^T$, $\chi_k = C \bar{\chi}_k^T$ and $F_{\alpha\beta} = \partial_\alpha A_\beta - \partial_\beta A_\alpha$.

Due to Majorana condition we get

$$\begin{aligned} \bar{\chi}_j \sigma_{\alpha\beta} \chi_k &= -\bar{\chi}_k \sigma_{\alpha\beta} \chi_j \\ \bar{\chi}_j \sigma_{\alpha\beta} \gamma_5 \chi_k &= -\bar{\chi}_k \sigma_{\alpha\beta} \gamma_5 \chi_j \end{aligned} \quad (2.2)$$

and so diagonal magnetic and electric dipole moment are forbidden (for Majorana neutrinos). Usually non diagonal moments are called transitional moments.

In the following we shall assume that some new interactions give rise to the effective Lagrangian (2.1) and we consider the possible effects.

§2.2 Neutrino evolution equation in a coherent magnetic field

The interaction of the neutrino with the magnetic field can lead to two different consequences

a) neutrinos are scattered by the field \mathbf{B} which is present in the convective zone.

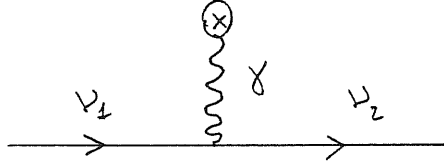
b) Some coherent effect of the same kind we have described in the previous chapter can hold.

We shall neglect *a* since it turns out that it requires unreasonable high value of μ and \mathbf{B} and we shall concentrate on *b*. Exactly in the same

manner as we got for the coherent weak interaction we get a contribution to the hamiltonian, due to the interaction of neutrino with the magnetic field; the coherent requirement leads exactly to the same condition: initial and final neutrino momentum must be equal.

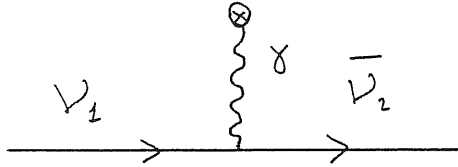
In presence of a coherent magnetic field the evolution hamiltonian has non vanishing elements wich connects ν_1^L and ν_2^L states with ν_2^R and ν_1^R states; therefore oscillations involving left handed and right handed componenents of both neutrino species are allowed.

For a static magnetic field, again using the convention of appendix A we get the followings forward scattering amplitudes



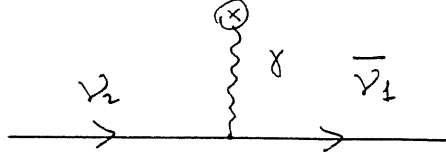
$$B_{1,2}^C = \frac{1}{2p\sqrt{(p_{01} + m_1)(p_{02} + m_2)p_{01}p_{02}}} \mathbf{pB}$$

$$\times [(p_{01} + m_1 - p)(p_{02} + m_2 + p)(\mu + id) + (p_{01} + m_1 + p)(p_{02} + m_2 - p)(\mu - id)]$$

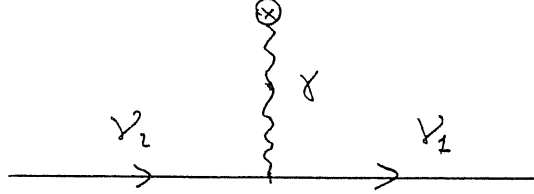


$$B_{1,2}^F = B e^{i\beta} \frac{1}{2p\sqrt{(p_{01} + m_1)(p_{02} + m_2)p_{01}p_{02}}}$$

$$\times [(p_{01} + m_1 + p)(p_{02} + m_2 + p)(\mu + id) + (p_{01} + m_1 - p)(p_{02} + m_2 - p)(\mu - id)]$$



$$\mathcal{B}_{2,1}^C = \mathbf{pB} \frac{1}{2p\sqrt{(p_{01} + m_1)(p_{02} + m_2)p_{01}p_{02}}} \\ \times [(p_{01} + m_1 + p)(p_{02} + m_2 - p)(\mu + id) \\ + (p_{01} + m_1 - p)(p_{02} + m_2 + p)(\mu - id)]$$



$$\mathcal{B}_{2,1}^F = -Be^{i\beta} \frac{1}{2p\sqrt{(p_{01} + m_1)(p_{02} + m_2)p_{01}p_{02}}} \\ \times [(p_{01} + m_1 + p)(p_{02} + m_2 + p)(\mu + id) \\ + (p_{01} + m_1 - p)(p_{02} + m_2 - p)(\mu - id)] \quad (2.3)$$

where $Be^{i\beta} = B_j + iB_k$, B_j and B_k being the components of the projection \mathbf{B}_\perp of the field \mathbf{B} in the plane transverse to neutrino momentum, and $(\mu + id) = \mu + id$. Including also this effect for the time evolution hamiltonian we get:

$$H_{TOT} = H_0 + \mathcal{V} + \mathcal{B} \quad (2.4)$$

Where H_0 stands for the kinetic term, \mathcal{V} and \mathcal{B} account for the coherent interactions of neutrinos with matter and magnetic field respectively.

$$H_{TOT} = \begin{pmatrix} \epsilon_1 + \mathcal{V}_{1,1} & \mathcal{V}_{1,2} + \mathcal{B}_{1,2}^C & 0 & \mathcal{B}_{1,2}^F \\ \mathcal{V}_{1,2}^* + \mathcal{B}_{1,2}^{C*} & \epsilon_2 + \mathcal{V}_{2,2} & -\mathcal{B}_{1,2}^F & 0 \\ 0 & -\mathcal{B}_{1,2}^{F*} & \epsilon_1 + \mathcal{V}_{1,1}^R & -(\mathcal{V}_{1,2}^* + \mathcal{B}_{1,2}^{C*}) \\ \mathcal{B}_{1,2}^{F*} & 0 & -(\mathcal{V}_{1,2} + \mathcal{B}_{1,2}^C) & \epsilon_2 + \mathcal{V}_{2,2}^R \end{pmatrix} \quad (2.5)$$

§2.3 The parameter region relevant for the solar neutrinos

Just to estimate the order of magnitude of the required μ and B we neglect \mathcal{V} and ϵ_j . For relativistic neutrinos $\mathcal{B}_C \ll \mathcal{B}_F$. With this approximation the relevant hamiltonian for an incoming ν_e is

$$\frac{i\partial}{\partial R} \begin{pmatrix} a_e \\ a_{\bar{\mu}} \end{pmatrix} = \begin{pmatrix} 0 & (\mu + id)Be^{i\beta} \\ (\mu - id)Be^{-i\beta} & 0 \end{pmatrix} \begin{pmatrix} a_e \\ a_{\bar{\mu}} \end{pmatrix} \quad (2.6)$$

Where a_e and $a_{\bar{\mu}}$ are the amplitude for ν_e and $\bar{\nu}_\mu$ content of the neutrino beam. From (66) we get for the probability $P_{e\bar{\mu}}$ to find a $\bar{\nu}_\mu$ at a distance R

$$P_{e\bar{\mu}} = \sin^2 \left| (\mu + id) \int_{R_i}^R dR B e^{i\beta} \right| \quad (2.7)$$

For $P_{e\bar{\mu}}$ to be significative we require

$$\left| (\mu + id) \int_{R_i}^{R_\odot} dR B e^{i\beta} \right| \geq 1 \quad (2.8)$$

Where R_i is the beginning of the convective zone and R_\odot is the solar radius. The length of the convective zone L_c is

$$L_c = \frac{3}{10} R_\odot \quad (2.9)$$

From (57) we get

$$\mu B \geq \frac{1}{L_c} \approx 10^{-15} eV \quad (2.10)$$

For magnetic field of order 1 up to 100 kG wich seems possible inside the convective zone of the sun this mean.

$$\mu_\nu \geq 2 \cdot 10^{-12} \div 2 \cdot 10^{-10} \mu_B \quad (2.11)$$

where μ_B is the Bohr magneton.

The upper value for μ_ν is at the border of the present terrestrial limit [21]. Astrophysical bounds are more stringent $\mu_\nu \leq 3 \times 10^{-12} \mu_B$ [22] even if some caution is needed. In any case, even being very optimistic about μ_ν and B values, from the experimental limit we get $\mu_\nu B \leq 10^{-14} eV$.

In general diagonal terms tend to suppress the spin flip precession [23] unless some resonance occur. Even if some adiabatic resonance occurs condition (2.12) still hold (up to factors of order unity).

Taking into account that in the convective zone

$$\frac{\mathcal{V}_{1,1} + \mathcal{V}_{2,2}}{2} \leq 5.5 \cdot 10^{-15} eV \quad (2.13)$$

We found that for getting appreciable effects $\epsilon_1 - \epsilon_2$ cannot exceed 10^{-14} eV. This means that even if we postulate that ν_e has a small admixture of a neutrino state with a large mass there is no chance to observe non relativistic entries in (2.5).

Neglecting term of order $\frac{m_\nu}{E_\nu}$ we get, in the flavour basis

$$H_{TOT} = \begin{pmatrix} \Delta \cos 2\alpha + \bar{\mathcal{V}}_1 & \Delta e^{i\delta} \sin 2\alpha & 0 & \mathcal{B} e^{i\theta} \\ \Delta e^{-i\delta} \sin 2\alpha & -\Delta \cos 2\alpha + \bar{\mathcal{V}}_2 & -\mathcal{B} e^{i\theta} & 0 \\ 0 & -\mathcal{B} e^{-i\theta} & \Delta \cos 2\alpha - \bar{\mathcal{V}}_1 & \Delta e^{-i\delta} \sin 2\alpha \\ \mathcal{B} e^{-i\theta} & 0 & \Delta e^{i\delta} \sin 2\alpha & -\Delta \cos 2\alpha - \bar{\mathcal{V}}_2 \end{pmatrix} \quad (2.14)$$

Where α has been defined in (1.2)

$$\mathcal{B} e^{i\theta} = (\mu + id) \mathcal{B} e^{i\beta}$$

$$\bar{\mathcal{V}}_1 = \frac{G}{\sqrt{2}} (2N_e - N_n)$$

$$\bar{\mathcal{V}}_2 = -\frac{G}{\sqrt{2}} N_n \quad (2.15)$$

θ and δ are CP violating phases. We now show that they are indeed irrelevant. Since we measure neutrino flavour content of the beam if a_x is the amplitude for the x neutrino content of the beam ($x = e, \mu, \bar{e}, \bar{\mu}$) to follow the evolution of a_x or of $A_x = e^{i\phi_x} a_x$ is completely equivalent.

This arbitrariness in the choice of phases is enough to remove the phases θ and δ from (2.15). Indeed with the choice

$$\begin{aligned} A_e &= a_e \\ A_\mu &= a_\mu e^{i\delta} \\ A_{\bar{e}} &= a_{\bar{e}} e^{i(\delta+\theta)} \\ A_{\bar{\mu}} &= a_{\bar{\mu}} e^{i\theta} \end{aligned} \tag{2.16}$$

we get the equation

$$i \frac{\partial}{\partial t} A_j = H_{(TOT)j,k} e^{i(\phi_j - \phi_k)} A_k = H'_{(TOT)j,k} A_k \tag{2.17}$$

and H'_{TOT} is real.

§2.4 The Hybrid models

In the original proposal of Okun, Voloshin and Visotky [20] it was assumed that ν_1 and ν_2 were the four component of a Dirac neutrino. In this case both Δ and the vacuum mixing angle are zero and the evolution hamiltonian in the $\nu_e, \bar{\nu}_x$ basis ($\nu_e, \bar{\nu}_x$ evolution is decoupled from $\nu_x, \bar{\nu}_e$ evolution) reduces to

$$\mathcal{H} = \begin{pmatrix} \mathcal{V}_1 & (\mu + id) B e^{i\beta} \\ (\mu - id) B e^{-i\beta} & \mathcal{V}_2 \end{pmatrix} \tag{2.18}$$

where \mathcal{V}_j take into account the coherent weak interaction.

However, at least if we take the more conservative assumption that the magnetic field is present only in the convective zone, (2.18) cannot account for any depletion at the minima of solar activity. Since a significant depletion is observed also at the minima of solar activity, it was natural to introduce models in which both neutrino mixing and spin precession were operative. These models which are defined by the evolution hamiltonian (2.5) are called Hybrid models [24].

We now study equation (2.6). Two situations can arise

- 1) some resonance can occur inside the convective zone
- 2) No resonance is crossed in neutrino travel.

In the following we shall show that 2 requires large mixing angle. This requirement leads to a large $\bar{\nu}_e$ production and conflict with experimental data.

If we assume that adiabatic resonances indeed occur this implies

$$5 \cdot 10^{-16} \text{eV} \leq \frac{m_1^2 - m_2^2}{4E} \leq 5 \cdot 10^{-15} \text{eV} \quad (2.19)$$

The diagonal element $H'_{j,j}$ of H'_{TOT} are depicted in the following fig.

2.

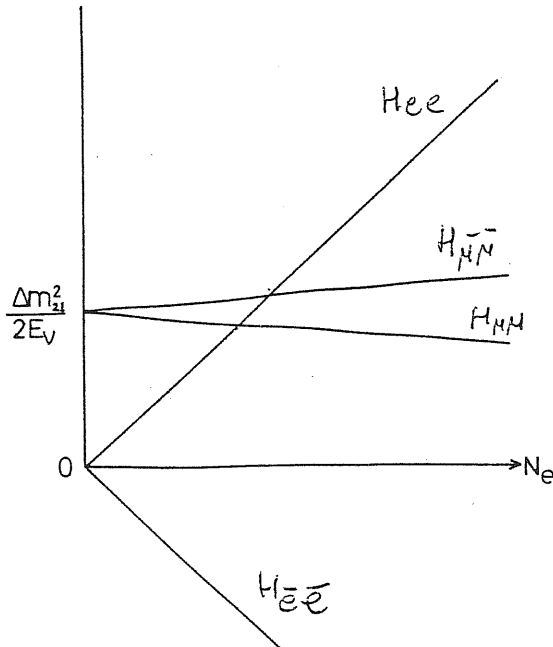


FIG. 2. The diagonal elements H_{xx} of the hamiltonian (2.14) as functions of electrons density.

We observe that in their travel neutrinos crosses two resonances, the first when $H_{ee} = H_{\bar{\mu}\bar{\mu}}$ which implies

$$\frac{G}{\sqrt{2}}(N_e - N_n) = \frac{m_1^2 - m_2^2}{4E} \quad (2.20)$$

if the crossing is adiabatic we have $\nu_e \rightarrow \bar{\nu}_\mu$ conversion.

The second crossing is for $H_{ee} = H_{\mu\mu}$ which implies

$$\frac{G}{\sqrt{2}}N_e = \frac{m_1^2 - m_2^2}{4E} \cos 2\alpha \quad (2.21)$$

Again if adiabaticity holds we have $\nu_e \rightarrow \nu_\mu$ conversion.

However it turns out that in the convective zone N_n is quite small ($N_n \approx 1/6N_e$) and the two resonance are very near, this implies that even when adiabaticity is a good approximation equation (2.6) requires numerical investigation.

To have some idea of the behaviour of the system we give some qualitative argument to follow neutrino evolution. Due to the resonance (2.20), (2.21) we expect a sizable amount of ν_μ and $\bar{\nu}_\mu$. In addition a small fraction of $\bar{\nu}_e$ is expected since it is not forbidden by any conservation law. It can be due to the following process

$$\begin{aligned} \nu_e &\xrightarrow{\text{spin flip}} \bar{\nu}_\mu \xrightarrow{\text{oscillation}} \bar{\nu}_e \\ \nu_e &\xrightarrow{\text{oscillation}} \nu_\mu \xrightarrow{\text{spin flip}} \bar{\nu}_e \end{aligned} \quad (2.22)$$

since in both process one step is not resonant the $\bar{\nu}_e$ fraction is expected indeed small if the mixing angle is small.

Some numerical investigation of (2.6) has been carried out [25] and it seems that this idea can reproduce experimental data accounting also for the observed difference between the two experiments. However due both to the incompleteness of this investigation and to our ignorance of magnetic field shape and size we still lack a quantitative knowledge of the allowed region for the parameters $(\mu_\nu, B, \alpha, \Delta m^2)$ and of the $\bar{\nu}_e$ flux.

In particular a better understanding of the following problems is needed:■

- a) The region of m and α which can reproduce the data.
- b) The dependence of the solution on the magnetic field shape.
- c) The relevance of the inner magnetic field
- d) The stability of the behaviour of the system for small change of the input parameters (especially $B(R)$).

§2.5 Additional experimental signaturee of the hybrid models

In the frame of the class of hybrid models we have described up to now some production of $\bar{\nu}_e$ is expected. Free proton rich detectors like

kamiokande are very sensitive to $\bar{\nu}_e$ and it is a meaningful effort to investigate what bounds the kamioka data put on the $\bar{\nu}_e$ productions and how significant are for the hybrid models [26].

§2.5.1 Bounds on the solar $\bar{\nu}_e$ flux from kamiokande background data

As is well known, the specific signature of $\bar{\nu}_e$ in materials containing hydrogen is through the reaction



which produces isotropically distributed monoenergetic positrons ($E_{e^+} = E_\nu - \delta m$, $\delta m = m_n - m_p$). For energies above a few MeV, the cross section is

$$\sigma(E_\nu) = 9.2 \times 10^{-42} \left[\frac{(E_\nu - \delta m)}{10 \text{ MeV}} \right]^2 \text{ cm}^2 \quad (2.23)$$

The Kamioka water detector, which is sensitive to the $\nu_e - e$ interaction with a much smaller cross section, is clearly also capable of detecting reaction (2.23) provided there is an appreciable flux of solar $\bar{\nu}_e$.

For the moment, we assume that the energy distribution of $\bar{\nu}_e$ is the same as that of ν_e apart for an overall factor $P(\bar{\nu}_e)$ denoting the probability of the $\nu_e \rightarrow \bar{\nu}_e$ transition. We also assume that the ν_e spectrum, $d\Phi/dE_\nu$, is that given by the standard solar model [3].

The average number of positron with energy larger than a threshold E_0 which are produced in the detector is

$$N(E_{e^+} \geq E_0) = P(\bar{\nu}_e) A T N_p \int_{E_0 + \delta m} dE_\nu \frac{d\Phi(SSM)}{dE_\nu} \sigma(E_\nu) \quad (2.24)$$

where T is the measurement time ($T = 1040$ days), N_p is the number of free protons contained in the fiducial mass of the Kamioka detector (680 tons of water) and A , an overall factor accounting for the SSM uncertainty, ranges in the interval $0.7 \div 1.3$.

This number is shown in table 1 (last column) for several values of E_0 , by taking $A = 1$ and $P(\bar{\nu}_e) = 1$. (In the same table, the number of $\nu_e - e$, $\bar{\nu}_e - e$, $\nu_\mu - e$ and $\bar{\nu}_\mu - e$ interactions are also shown for comparison.)

E_0 [MeV]	$N(E_{e^-} > E_0)$				
	$\nu_e - e$	$\bar{\nu}_e - e$	$\nu_\mu - e$	$\bar{\nu}_\mu - e$	$\bar{\nu}_e - p$
5.30	2.08×10^3	3.59×10^2	3.16×10^2	2.45×10^2	6.65×10^4
6.30	1.42×10^3	2.13×10^2	2.13×10^2	1.63×10^2	5.68×10^4
7.30	9.05×10^2	1.20×10^2	1.34×10^2	1.01×10^2	4.48×10^4
8.30	5.29×10^2	6.32×10^1	7.77×10^1	5.83×10^1	3.17×10^4
9.30	2.76×10^2	3.03×10^1	4.02×10^1	3.00×10^1	1.93×10^4
1.03×10^1	1.23×10^2	1.26×10^1	1.78×10^1	1.32×10^1	9.40×10^3
1.13×10^1	4.34×10^1	4.25	6.25	4.62	3.13×10^3
1.23×10^1	1.06×10^1	1.00	1.52	1.12	5.13×10^2
1.33×10^1	1.37	1.27×10^{-1}	1.96×10^{-1}	1.44×10^{-1}	2.24×10^1

TABLE 1.

Average number of interactions taking place within Kamiokande II fiducial volume during $T=1040$ d. with energy of e^\pm in excess of E_0 by assuming for each neutrino species the same differential flux $d\Phi/dE_\nu$ as given by the SSM for ν_e and by taking $\sin^2 2\theta_W = 0.23$.

If we take $E_0 = 9.3$ MeV, the detection efficiency for e^- exceed 90 % [27]. We assume the efficiency for e^+ to be the same, thus the average number of detected positrons is

$$N^{det}(E_{e^+} \geq E_0) \geq AP(\bar{\nu}_e) \times 1.7 \times 10^4 \quad (2.25)$$

These events, being isotropically distributed, contribute to the flat background detected by Kamioka in the angular distribution. On the other hand, the total background for 1040 days at $E_0 = 9.3$ MeV is about 1160 counts, see fig. 3 of ref. [19]. This provides a bound on $N_{det}(E_{e^+} \geq E_0)$ and thus on $AP(\bar{\nu}_e)$:

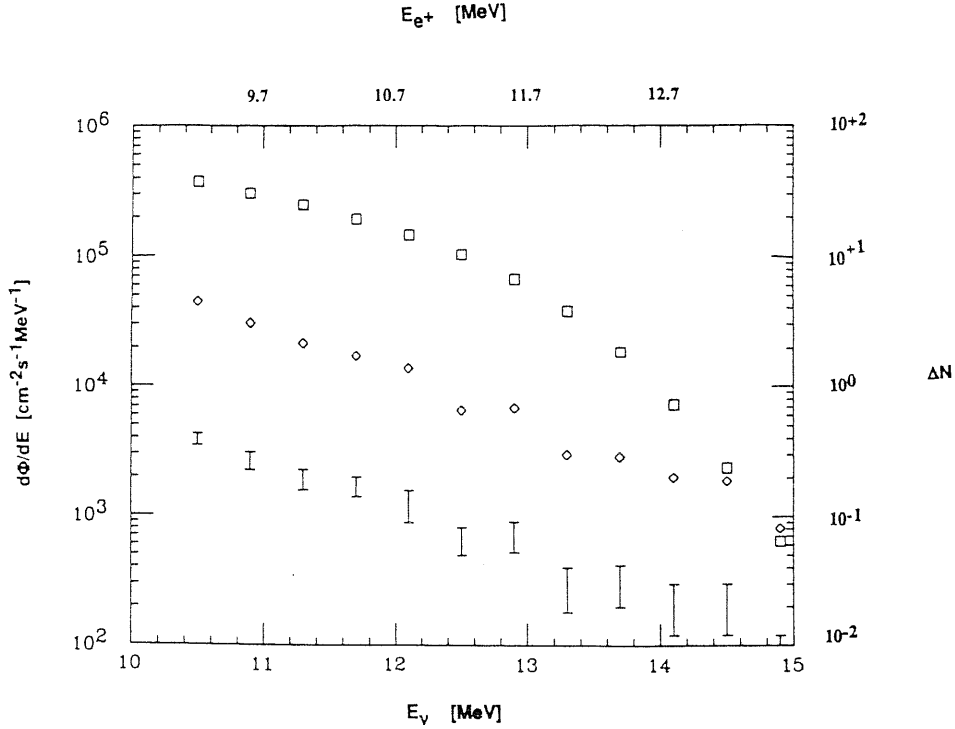
$$A(P(\bar{\nu}_e)) \leq 7.7\% \quad (\text{at } 99\% \text{ CL}) \quad (2.26)$$

where the average refers to the data taking period January 1987 - April 1990.

More detailed information can be obtained by looking at the energy distribution of the Kamiokande events, see fig.3 (vertical bars) from ref [28], corresponding to the period June 1988 - April 1989. The number of positrons which are produced inside the detector in the energy interval $E_{e^+} \div E_{e^+} + \Delta E$ in time Δt is given by

$$\frac{\Delta N_{e^+}}{\Delta E \Delta T} = N_p \sigma(E_\nu) \frac{d\Phi_{\bar{\nu}}}{dE_\nu} \quad (2.27)$$

where $E_{e^+} = E_\nu - \delta m$ and $d\Phi_{\bar{\nu}}/dE_\nu$ is the flux of $\bar{\nu}$ which we want to determine. Again by assuming a detection efficiency better than 90% and requiring that the number of detected positrons does not exceed the observed signal, we get the upper bound for $d\Phi_{\bar{\nu}}/dE_\nu$ shown in fig. 3 (diamonds).



The background spectrum in the Kamiokande II experiment for the period June 1988 - April 1989 [28], in units of counts ΔN per day per energy interval of 0.4 MeV (vertical bar, right scale) as a function of the electron or positron energy $E_{e\pm}$ (top scale). The corresponding upper bound on the $\bar{\nu}_e$ flux (diamonds, left scale), differentiated with respect to neutrino energy E_ν (bottom scale), fixed at $E_\nu = E_{e\pm} + \delta m$. For comparison, the differential flux of ν_e predicted by the SSM is also shown (squares).

We derive that the total flux of $\bar{\nu}_e$ in the energy region of interest to us is severely bound,

$$\Phi_{\bar{\nu}}(E_\nu \geq 10.6\text{MeV}) \leq 6.1 \times 10^4 \text{cm}^{-2} \text{s}^{-1} \quad \text{at 99\%CL} \quad (2.28)$$

in comparison with the $\bar{\nu}_e$ flux predicted by the SSM in the same region $\Phi(SSM)(E_\nu \geq 10.6\text{MeV}) = A \times 6 \times 10^5 \text{cm}^{-2} \text{s}^{-1}$.

We remark that the bound in eq. (2.28) does not depend on assumptions about the spectrum of the antineutrinos. A more stringent bound can

be derived if one assumes, as above, the spectrum to be the same as for ν_e . One finds in this way

$$A\langle P(\bar{\nu}_e) \rangle \leq 6\% \quad (\text{at } 99\% \text{CL}) \quad (2.29)$$

§2.5.2 Hybrid models with large mixing angles and solar $\bar{\nu}_e$ flux

With the aim of appreciating how severe are the bounds we presented, we discuss as a concrete example a simple hybrid model, where we assume:

a) validity of the SSM

b) a squared neutrino mass difference $\delta m^2 = 10^{-9} \text{eV}^2$, so that the oscillation length $\lambda = 4\pi E_\nu / \delta m^2$ is much larger than the solar radius and much smaller than the sun earth distance ($E_\nu \simeq 10 \text{MeV}$)

c) a $\nu_e \rightarrow \bar{\nu}_\mu$ transition magnetic moment, $\langle \nu_e | \mu | \bar{\nu}_\mu \rangle$, and a transverse magnetic field B in the convective zone of the Sun such that, when the solar activity is high, the magnetic interaction energy $E_M = \mu B$ is the dominant term of the neutrino evolution hamiltonian in the convective zone:

$$E_M \gg \frac{\delta m^2}{E_\nu} \quad E_M \gg G n_e \quad (2.30)$$

where n_e is the electron density and G is the Fermi constant.

Independently of E_ν for each ν_e produced in the core of the sun the probabilities of emerging from the surface of the sun as ν_e and $\bar{\nu}_\mu$ are respectively

$$P_S(\nu_e) = \cos^2 \beta, \quad P_S(\bar{\nu}_\mu) = \sin^2 \beta \quad (2.31)$$

where $\beta = \mu \int dr B(r)$ and the integral is between the beginning and the end of the convective zone. It is natural to take B to be proportional to the square root of the sunspot number N_{ss} [29], so that

$$\beta = f\sqrt{N_{ss}} \quad (2.32)$$

In the trip from the sun to the earth a flavour transition can occur with an average probability $\sin^2 \theta$, which can be written in terms of the vacuum mixing angle α as

$$\sin^2 \theta = \frac{1}{2} \sin^2(2\alpha) \quad (2.33)$$

In conclusion, the arrival probabilities of the different neutrino species can be written as

$$\begin{aligned} P(\nu_e) &= \cos^2 \theta \cos^2(f\sqrt{N_{ss}}) \\ P(\bar{\nu}_e) &= \sin^2 \theta \sin^2(f\sqrt{N_{ss}}) \\ P(\nu_\mu) &= \sin^2 \theta \cos^2(f\sqrt{N_{ss}}) \\ P(\bar{\nu}_\mu) &= \cos^2 \theta \sin^2(f\sqrt{N_{ss}}) \end{aligned} \quad (2.34)$$

We can now get information on the two parameters θ and f by analysing the experimental data of the Kamioka experiment.

For high electron energy threshold (E_0 close to the kinematical bound) the cross section of $\nu_e - e$, $\bar{\nu}_e - e$ and $\bar{\nu}_\mu - e$ are about 1/9 of the $\nu_e - e$ cross section (within 20%), see for example table 1. In the Kamioka experiment, the ratio R_K of the electron signal in the direction opposite to the sun to the expectation of the SSM can be written as

$$R_K = A\{P(\nu_e) + \frac{1}{9}[1 - P(\nu_e)]\} = A\left[\frac{8}{9} \cos^2 \theta \cos^2(f\sqrt{N_{ss}}) + \frac{1}{9}\right] \quad (2.35)$$

For simplicity, and without affecting the results in any significant way, we make a two parameter fit of these data by assuming

$$R_K = \frac{8}{9}C \cos^2(f\sqrt{N_{ss}}) + \frac{1}{9} \quad (2.36)$$

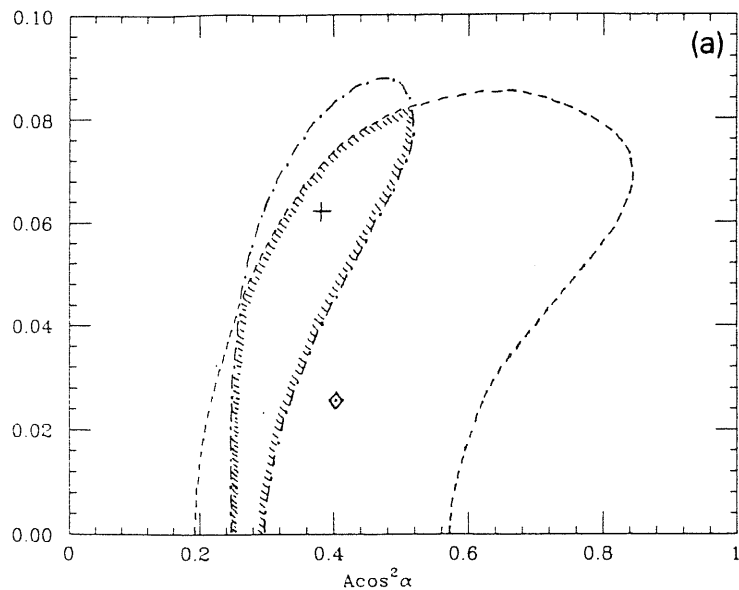
where $C = A \cos^2 \theta$

The available data on R_K correspond to five time intervals in the period 1987 - 1990, see fig. 2 of ref. [19]. Fig. 4 shows in the plane (C, f) the results of the best fit (diamond) and the 99% CL contour (dashed curve).

The Chlorine experiment can be analyzed in the same way. The ratio of the observed number of Ar^{37} atoms to the expectation of the SSM is

$$R_{Cl} = C \cos^2(f\sqrt{N_{ss}}) \quad (2.37)$$

By analysing the Chlorine data for the period 1970 - 1990 (and by treating the quoted errors as if they were up - down symmetrical) we find as best fit value the point denoted by the cross in fig. 4 and at the 99% CL the area inside the dot - dashed curve. The shaded area denotes the area in the (C, f) plane consistent with both experiments.

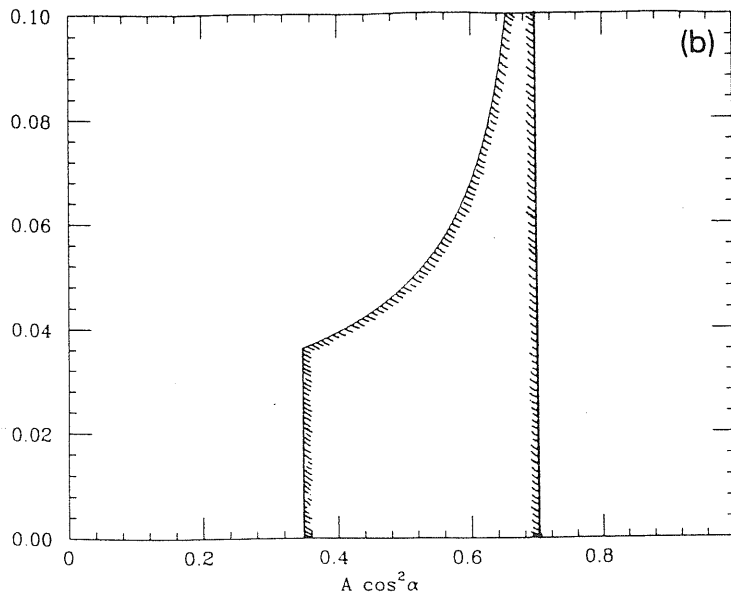


In the plane ($C = A \cos \alpha, f$) we show the best fit for Kamiokande II electron signal R_K in the period 1987 - 1990 (diamond) and the allowed region (inside the dashed curve), the best fit of the Ar^{37} signal R_D in the period 1970 - 1990 (cross) and the allowed region (inside the dot-dashed curve), and we show the region which is consistent with the above constraint within the shaded curve. All curves correspond to 99 % confidence level

By using eq. (2.34), the upper bound on the fraction of $\bar{\nu}_e$ given in eq (2.29) can be written as

$$(A - C) \langle \sin^2(f \sqrt{N_{ss}}) \rangle_{88-89} < 6\% \quad (2.38)$$

In fig. 5 this constraint corresponds to the region below the full curve, for $A = 0.7$. Also shown, for the same value of A , is the constraint arising from eq. (2.33), $\cos^2 \theta > 0.5$ or $C > 0.35$.



The boundary of the region corresponding to the upper bound on the $\bar{\nu}_e$ flux (full curve), calculated for $A = 0.7$, the constraint $0.5 < \cos^2 \theta < 1$ (vertical lines) and the region consistent with the above constraints (shaded area).

No region of parameter space is left which is consistent both with the signal in the Chlorine experiment and in the Kamioka experiment as well as with the indirect information on the $\bar{\nu}_e$ flux. Choosing a value of A greater than 0.7 would worsen the situation.

The discussion of the simple model given above shows that, when building a consistent hybrid model, one has to avoid overproduction of $\bar{\nu}_e$. This can be accomplished, perhaps, by exploiting resonant phenomena induced by matter effects, for a suitable choice of parameters of the model [30]. Alternatively, a complete suppression of $\bar{\nu}_e$ can be achieved in a class of hybrid models where a suitable combination of lepton numbers (e.g. $L_e + L_\mu - L_\tau$) is conserved. We will come back to this last possibility in the next chapter.

Other mechanism of $\bar{\nu}_e$ production occur in a class of models where a heavy neutrino decay into a lighter one and in a pseudoscalar $\nu_2 \rightarrow \bar{\nu}_1 + M$. The most characteristic feature of all neutrino decay scenarios (including the matter induced decay) is that the $\bar{\nu}_e$ takes a smaller fraction of the initial neutrino energy, typically 1/3. The data we have discussed (corresponding to a threshold energy of 9.3 MeV) are clearly poor for giving information on the decay process. On the other hand, interesting information could be obtained with a significantly lower detection threshold.

CHAPTER 3

NEUTRINO OSCILLATION AND MAGNETIC MOMENT TRANSITION IN A MODEL WITH A CONSERVED LEPTON NUMBER

As we have already stressed the hybrid models proposed up to now, in our opinion, present two unpleasant features: they require two vastly different mass scales [31] and they lead to the production of $\bar{\nu}_e$, which are severely restricted by data. A natural way of avoiding both these problems [32] consists in considering all the three standard neutrino flavours ν_e , ν_μ and ν_τ and assuming a suitable nonstandard lepton number to be conserved:

$$L_\pm = L_e \pm L_\mu \mp L_\tau \quad (3.1)$$

This conservation law implies just one mass scale, the mass spectrum consisting of one massive Dirac neutrino and one massless Weyl neutrino [33]. An unquenched magnetic transition can take place between the two helicity states of the Dirac neutrino and, on the other hand, the fact that the mass eigenstates are linear superpositions of the different neutrino flavours gives rise to a flavour oscillation. In other words by considering all the three neutrino flavours one can have flavour oscillations even in the presence of a Dirac neutrino state in the spectrum.

§3.1 The model

For definiteness, we take L_+ as a conserved quantum number. The most general mass term which is consistent with this constraint is

$$\mathcal{L}_m = -m\bar{\nu}_{\tau R}^C (\nu_{eL} \cos \alpha + \nu_{\mu L} \sin \alpha) + h.c. \quad (3.2)$$

This lagrangian describes one Dirac neutrino with mass m

$$\psi_{mL} = \nu_{eL} \cos \alpha + \nu_{\mu L} \sin \alpha, \quad \psi_{mR} = \nu_{\tau R}^C \quad (3.3)$$

and a massless Weyl neutrino

$$\nu_0 = -\nu_{eL} \sin \alpha + \nu_{\mu L} \cos \alpha \quad (3.4)$$

For a sizeable values of the mixing angle α , experiment at nuclear reactors yield [34] $m \leq 0.1$ eV. Since significant magnetic moments call for high masses, we will explore the region near this upper bound

$$m \approx 10^{-2} - 10^{-1} \text{ eV} \quad (3.5)$$

In this range of masses the existing data from accelerator experiments on $\nu_e \rightarrow \nu_\mu$ ($\bar{\nu}_e \rightarrow \bar{\nu}_\mu$) do not impose any constraint on α .

The most general magnetic moment effective lagrangian, consistent with the conservation of L_+ , has the form

$$\mathcal{L}_\mu = -\frac{1}{2} \mu \nu_{\tau R}^C \sigma_{\lambda\phi} F_{\lambda\phi} (\nu_{eL} \cos \beta + \nu_{\mu L} \sin \beta) + h.c. \quad (3.6)$$

The Hamiltonian H wich determines the evolution of the ν_e state in the sun

$$i \frac{\partial}{\partial r} | \nu(r) \rangle = H(r) | \nu(r) \rangle \quad (3.7)$$

where $r = ct$, is immediately obtained from eqs. (3.2) and (3.6), including the coherent neutrino weak interaction with matter [16]. We observe that due to the conserved lepton number the hamiltonian decouples into two sub-hamiltonians each couplings only three states. In the mass eigenstates basis ($| \nu_0 \rangle, | \psi_{mL} \rangle, | \psi_{mR} \rangle$) one has

$$H(r) = \begin{pmatrix} G_F n_e \sqrt{2} \sin^2 \alpha - \frac{G_F n_n}{\sqrt{2}} & -G_F n_e \sqrt{2} \cos \alpha \sin \alpha & \mu B \sin(\beta - \alpha) \\ -G_F n_e \sqrt{2} \cos \alpha \sin \alpha & \frac{m^2}{2E} + G_F n_e \sqrt{2} \cos^2 \alpha - \frac{G_F n_n}{\sqrt{2}} & \mu B \cos(\beta - \alpha) \\ \mu B \sin(\beta - \alpha) & \mu B \cos(\beta - \alpha) & \frac{m^2}{2E} + \frac{G_F n_n}{\sqrt{2}} \end{pmatrix} \quad (3.8)$$

where n_e and n_n are the electron and neutron densities respectively, G_F is the Fermi constant and $B = B(r)$ is the transverse component of the solar magnetic field.

In the convective zone ($r \geq R_B = 0.7R_\odot$, where $R_\odot = 7 \times 10^5$ km is the solar radius) we assume $n_n = 1/6n_e$ and the density profile to be given by [3]

$$n_e \approx n_0 \exp\left(\frac{-r}{L_m}\right) \quad (3.9)$$

with $L_M \approx 0.1R_\odot$, and $n_e(R_B) \approx 0.16 N_A \text{cm}^{-3}$, N_A being the Avogadro number.

Concerning the magnetic field, we will assume that it is confined within the convective zone. In the absence of detailed information on the shape of the field, we use the following parametrization:

$$B(r) = \theta(r - R_B) B_0 \left\{ 1 - \exp\left[\frac{-r + R_B}{L_B}\right] \right\} \quad (3.10)$$

The starting point R_B is taken at the beginning of the convective zone. The raising length L_B (some fraction of the convective zone) and the plateau value B_0 are kept as free parameters. B_0 varies during the solar cycle, from $B_0 \approx 0$ at the solar minima up to a value B^{max} in correspondence of the maxima of the solar activity.

Note that according to (3.10), in the very outer region of the sun the field does not fall (as fast) as the coherent weak interaction. In fact we

expect the magnetic field to decrease with some power of the distance, whereas the density profile is exponentially decaying.

It is useful to introduce a magnetic energy term,

$$\epsilon(r) = \mu B(r) \cos(\beta - \alpha) \quad (3.11)$$

and a magnetic energy plateau ϵ_0 which is obtained from (3.11) for $B = B_0$. For the values of interest to us ($\mu \approx 10^{-10} \mu_B$, $B_0^{max} \approx 1 T$) one has $\epsilon_0^{max} \approx 20/R_\odot$ for $\cos(\beta - \alpha) = 1$.

§3.3 Flavour oscillations and spin flip in the absence of coherent weak interaction

As a first stage of the discussion, we neglect in eq. (3.8) the coherent weak interactions. For the values of interest to us, one has $m^2/2E \gg \mu B$ and consequently the $|\nu_0\rangle$ state is decoupled from the others.

One also has $(m^2/2E)R_\odot \gg 1$ and so the oscillating terms of argument $(m^2/2E)R_\odot$ can be replaced by their average values. In these hypothesis, the arrival probability $P(\nu_x)$ of the originally ν_e state are

$$\begin{aligned} P_{ee} &= \sin^4 \alpha + \cos^4 \alpha \cos^2 \Phi \\ P_{e\mu} &= \frac{1}{4} \sin^2 2\alpha (1 + \cos^2 \Phi) \\ P_{e\bar{\tau}} &= \cos^2 \alpha \sin^2 \Phi \\ \Phi &= \mu \cos(\beta - \alpha) \int dr B(r) \end{aligned} \quad (3.12)$$

The main phenomenological features of the model are immediate from the equations given above:

a) Let us assume that the spectrum of neutrinos produced in the core of the sun dF/dE , is correctly given by the standard model, apart from a factor A accounting for the SSM uncertainties:

$$\frac{dF}{dE} = A \frac{dF^{SSM}}{dE}, \quad A = 0.7 \div 1.3 \quad (3.13)$$

In this case, the ratio of the signal in the Chlorine experiment to the expectation of the SSM is simply

$$R_C = AP_{ee} \quad (3.14)$$

The signal deficit at solar minima ($\Phi = 0$) calls for a large value of the vacuum mixing angle. Indeed from eqs. (VII) and (3.12) at the 1σ level, one gets

$$2\left(1 - \frac{0.61}{A}\right) \leq \sin^2 2\alpha \leq 2\left(1 - \frac{0.45}{A}\right) \quad (3.15)$$

In the case $A = 1$ this yields

$$0.78 \leq \sin^2 2\alpha \leq 1 \quad (3.16)$$

Note that the same result hold for $\Phi = 0$ also in the case that coherent weak interactions are included. In other words, the signal deficit at solar minima always implies a large vacuum mixing angle.

b) A significant depletion of the signal in correspondence of the solar maxima can be achieved only for Φ_{max} close to $\pi/2$. In fact, smaller values of Φ_{max} yield a too small time dependence, whereas for larger values the signal oscillates with a frequency larger than that of the solar cycle. As remarked in [35] this condition requires a fine tuning of the parameters (μ and B) which are involved.

c) Even for the best case, $\Phi_{max} = \pi/2$, a significant depletion of the signal at the solar maxima calls for large vacuum mixing angle. From (VII) one has

$$\frac{\langle R_D \rangle_{max}}{\langle R_D \rangle_{min}} = 0.19 \pm 0.07 \quad (3.17)$$

By using eq (3.12) with $\Phi_{max} = \pi/2$ and $\Phi_{min} = 0$ we get, at the 1σ level

$$\sin^2 2\alpha = 0.79 \pm 0.20 \quad (3.18)$$

d) In the Kamioka experiment, in addition to ν_e , both ν_μ and $\bar{\nu}_\tau$ can scatter off electrons. For the Kamioka experiment one has

$$R_K = A[P_{ee} + W_\mu(E_{th})P_{e\mu} + W_\tau P_{e\bar{\tau}}] \quad (3.19)$$

where the factors $W_x(E_{th})$ depend on the threshold energy and on neutrino flavour (for $E_{th} = 9.3$ MeV $W_\mu = 1/7$ and $W_\tau = 1/9$. For the present model one obviously have $\langle R_K \rangle > \langle R_D \rangle$, in agreement with the trend of the experimental data. Also, the time modulation comes out to be weaker in Kamioka. As an example, by assuming $\Phi_{max} = \pi/2$ and $\Phi_{min} = 0$ at solar maxima and minima respectively, for α as in (3.18) and threshold energy $E_{th} = 9.3$ MeV we get a modulation $\langle R_K \rangle_{max} / \langle R_K \rangle_{min} = .34 \pm .06$

§3.4 Inclusion of coherent weak interaction

The neutrino evolution corresponding to the full hamiltonian given in eqs (3.8) has to be studied numerically. In this section we shall investigate two opposite limiting cases, wich can be discusses analitically and yield a qualitative understanding of the complete solution.

For the values of masses we are considering (see (3.5)) both Gn_e and Gn_n are (almost) negligible in comparison with the energy splitting, $m^2/2E$. The same holds true for the μB term for the values of interest to us. In these circumstances, the massless neutrino component $|\nu_0\rangle$ is practically decoupled from the others.

The problem thus simplifies to the study of a two state system, $|\psi_{mL}\rangle$ and $|\psi_{mR}\rangle$. For this system the relevant part of the hamiltonian (i. e. apart from terms proportional to the identity) is

$$h(r) = \begin{pmatrix} \Delta(r) & \epsilon(r) \\ \epsilon(r) & -\Delta(r) \end{pmatrix} \quad (3.20)$$

where

$$\frac{\Delta(r)}{\sqrt{2}} = G(n_e \cos^2 \alpha - n_n) \quad (3.21)$$

Note that, since the magnetic moment couples the left and the right components of the same Dirac neutrino, there are no mass terms inhibiting the spin flip transition.

We recall that we assume a large mixing angle $\cos^2 \alpha \approx 1/2$ and in the convective region we use eq. (3.9). We note that, as a consequence of the large vacuum mixing angle, $\Delta(r)$ never vanishes in the convective zone. A non zero value of $\Delta(r)$ clearly inhibites spin flip transitions [14], with respect to the case without coherent weak interactions.

The term $\epsilon(r)$ is defined by means of eqs. (3.10) and (3.11)

$$\epsilon(r) = \theta(r - R_B)\epsilon_0 \left\{ 1 - \exp\left[-\frac{-r + R_B}{L_B}\right] \right\} \quad (3.22)$$

We shall investigate the solution of the problems in terms of the field raising distance L_B and the interactio energy plateau ϵ_0 wich, we recall,

varies during the solar cycle from $\epsilon_0 \approx 0$ at solar minima up to a maximum value ϵ_0^{max} at solar maxima.

Qualitatively, for the solution of the problem, one can distinguish three different regions:

a) in the inner part of the sun (say $r < R_1$) weak coherent effects dominate ($\Delta(r) \gg \epsilon(r)$) and the solution is immediate. For a state which is $|\psi_{mL,R}\rangle$ at $r = 0$ one has

$$r < R_1 : \quad |\psi_{mL,R}\rangle \rightarrow |\psi_{mL,R}\rangle \exp(\pm i \int^r ds \Delta(s)) \quad (3.23)$$

b) In the outer part (say $r > R_2$) the magnetic moment interactions dominates ($\Delta(r) \ll \epsilon(r)$). Also in this case the analytical solution is immediate. For a state which can be described as $|\psi_{mL,R}\rangle$ at $r = R_2$ one has

$$\begin{aligned} r > R_2 : \quad & |\psi_{mL}\rangle \rightarrow |\psi_{mL}\rangle \cos \xi(r) - i |\psi_{mL}\rangle \sin \xi(r) \\ & |\psi_{mR}\rangle \rightarrow -i |\psi_{mL}\rangle \sin \xi(r) + |\psi_{mR}\rangle \cos \xi(r) \\ & \xi(r) = \int_{R_2}^r ds \epsilon_B(s) \end{aligned} \quad (3.24)$$

c) In the intermediate region $R_1 < r < R_2$, Δ and ϵ are comparable. The behaviour of the solution in this intermediate region (and consequently of the entire problem) depends crucially on the shape of the magnetic field. One can envisage two limiting situations, corresponding respectively to an adiabatic or a sudden transition between regions *a* and *b*. We investigate the region of validity of the two approximations in the plane (ϵ_0, L_B) and then we discuss the appropriate solution for both cases.

§3.4.1 The adiabatic and the sudden region

The transition between the two regions can be taken as adiabatic or sudden depending on the value of the function

$$g(r) = \frac{|\epsilon\Delta' - \epsilon'\Delta|}{2(\epsilon^2 + \Delta^2)^{3/2}} \quad (3.25)$$

For $g \ll 1$ ($g \gg 1$) the adiabatic (sudden) limit is realized. One has to verify such condition close to the point $r = r^*$ where $\epsilon(r^*) = \Delta(r^*)$. the curves shown in fig. 6 correspond, for $\cos^2 \alpha \approx 1/2$, to $g(r^*) = 1$, i. e. they denote the transition between the two regimes.

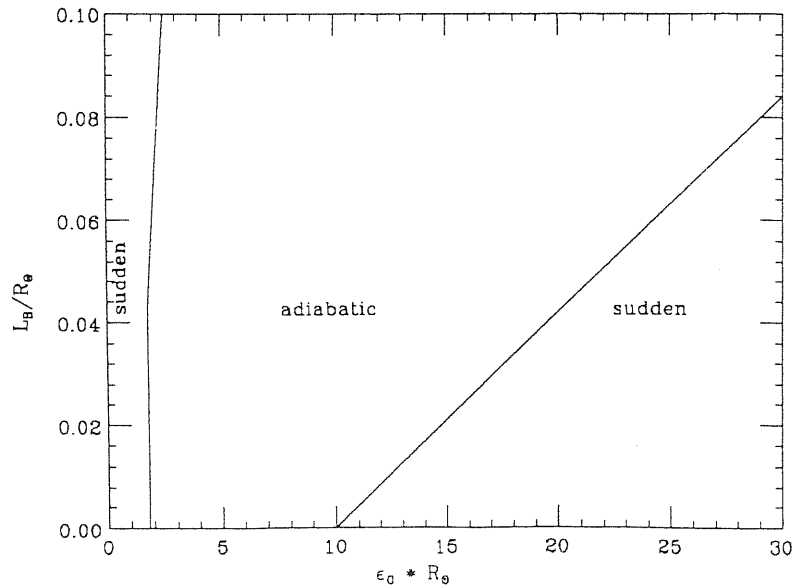


FIG. 6 In the plane (ϵ_0, L_B) we show the borders of the adiabatic and the sudden regimes, defined as $g = 1$, see eq. (3.25). ϵ_0 is the plateau value of the magnetic interaction energy and L_B is its raising length. R_\odot is the solar radius.

The main features of fig. 6 can be understood from the following considerations. Note that g is the sum of two positive functions, $g = g_1 + g_2$,

where

$$g_1(r) = -\frac{\epsilon\Delta'}{2(\epsilon^2 + \Delta^2)^{3/2}} \quad g_2(r) = -\frac{\epsilon'\Delta}{2(\epsilon^2 + \Delta^2)^{3/2}} \quad (3.26)$$

At $r = r^*$, $g_1 = [4\sqrt{2}L_M\epsilon(r^*)]^{-1}$ and one has $g_1 \geq 1$ for $\epsilon_0 \leq (4\sqrt{2}L_M)^{-1}$. This explains the region of small fields where the sudden limit is achieved.

For intermediate values of the field, $(4\sqrt{2}L_M)^{-1} \leq \epsilon_0 \leq \Delta(r_B) \approx 10/R_\odot$, g_1 is smaller than unity. Also, the magnetic interaction ϵ approaches its plateau value ϵ_0 before r^* and $g_2(r^*)$ tend to zero. Consequently the adiabatic condition can be satisfied. For even larger fields ($\epsilon_0 \geq \Delta(r_B) \approx 10/R_\odot$) r^* is reached while the magnetic interaction energy ϵ is raising and the adiabatic condition is fulfilled only for sufficiently large values of L_B .

§3.4.2 The adiabatic and the sudden solution

If the transition between regions a and b is adiabatic, the (instantaneous) eigenstates of region a go into the corresponding ones of the region b . After traversing the sun the probabilities of the different neutrino flavours are

$$\begin{aligned} P_{ee} &= \sin^4 \alpha + \frac{1}{2} \cos^4 \alpha \\ P_{e\mu} &= \frac{3}{8} \sin^2 2\alpha \\ P_{e\bar{\tau}} &= \cos^2 \alpha \end{aligned} \quad (3.27)$$

where oscillating terms of argument $(m^2/2E)R_\odot \gg 1$ have been averaged. If the transition is sudden, when crossing the intermediate region ($R_1 < r < R_2$) the $|\psi_{mL,R}\rangle$ states do not change. Beyond R_2 , coherent interactions are

irrelevant and the time evolution is the same as discussed in the previous section.

The arrival probabilities are thus given again by eqs. (3.12), where the phase Φ is now given by

$$\Phi = \mu \cos(\beta - \alpha) \int_{R_2} ds B(s) \quad (3.28)$$

This means that the magnetic field contributes to the phase only in the region where it overwhelms the coherent weak interaction.

§3.4.3 Discussion

On these grounds we can discuss the arrival probabilities P_{ex} during the different phases of the solar cycle.

For any L_B , at the solar minimum ($\epsilon_0 \approx 0$) one is in the sudden limit. The solution is given by eqs (3.12) with $\Phi = 0$. As discussed in section (3.3) a significant depletion of the neutrino signal can be obtained for large mixing angles, as given in eq. (3.16).

As the field raises, different regimes (adiabatic, sudden, or intermediate) can be reached depending on the value of ϵ_0^{max} and L_B .

From the phenomenological point of view, the most important features of the adiabatic regime are:

a) The results do not depend on the precise value of μ and B_0^{max} . Thus a significant modulation of the signal, anticorrelated with the solar cycle, can be obtained without a fine tuning of the magnetic field and magnetic moment, provided that ϵ_0^{max} and L_B .

b) Note that the lowest values of ϵ_0^{max} which satisfy the adiabatic condition (and thus provide a significant time modulation) are of order

$\epsilon_0^{max} \approx 5/R_\odot$, (the inverse of the convective zone dimension). Whichever mechanism one is invoking, one cannot do better, in the sense that for a significant spin flip probability the phase $\Theta = \epsilon_0 D$ where D is the depth of the convective zone, has to exceed unity.

c) On the other hand, the minimum value of P_{ee} is $1/3$, which is at the border of the region allowed by the Chlorine data. Also, the signal modulation in the Chlorine experiment $\langle R_C \rangle_{max} / \langle R_C \rangle_{min}$ cannot be smaller than one half, which looks in disagreement with (VII).

In the case that sudden regime is reached, the same phenomenological consideration as for the "vacuum" case hold. In addition, we note that only the region of high fields ($\epsilon_0 > 10/R_\odot$) is relevant for getting a significant phase Φ . In comparison with the adiabatic limit, the sudden case requires ϵ_0^{max} appreciably larger in order to achieve a significant time modulation. On the other hand, the amplitude of the modulation can be much larger, as previously remarked.

In summary, the inclusion of matter effects does not alter drastically the picture. One can choose the available parameters so as to reproduce the main feature of experimental results. Furthermore, if adiabaticity holds, one has a natural suppression of the signal at the solar maxima, which does not require a fine tuning of the neutrino magnetic moment and the solar magnetic field.

So far we restricted the magnetic field to the convective zone. On the other hand, the existence of a primordial field in the core of the sun, B_{in} is not excluded. Of course B_{in} is decoupled from the eleven years solar semicycle. Before closing this section we note a peculiarity which occurs for $B_{in} \neq 0$. For $\cos^2 \beta < 1/2$, $\Delta(r)$ reverses its sign in the core of the sun. If the resonance is crossed adiabatically all $|\psi_{mL}\rangle$ transform into $|\psi_{mR}\rangle$. In the convective zone, if the field is high enough, the $|\psi_{mR}\rangle$ transform

back into $|\psi_{mL}\rangle$. Thus a positive correlation with the magnetic field would occur.

§3.4.4 Conclusions

We have developed a phenomenological model with both neutrino flavour oscillations and spin flip transitions, characterized by a lepton number conservation law $L_{\pm} = L_e \pm L_{\mu} \mp L_{\tau}$. This implies a massless Weyl neutrino and one massive Dirac neutrino. The main consequences of this class of models are:

i) There is a large mixing angle between ν_e and ν_{μ} or ν_{τ} depending on the choice of the conserved lepton number (L_+ or L_-).

ii) The mass difference Δm coincides with the mass of the Dirac neutrino. As such it cannot be too small, in order to allow for a sizable magnetic moment. A value of order $10^{-1} \div 10^{-2}$ eV is consistent with bounds from reactor experiments. We note that $\nu_e - \nu_{\mu}$ oscillation with a large mixing angle and similar Δm may be indicated by the recently reported atmospheric neutrino flux anomaly [36].

iii) We have seen that the model can account for both the experimental data of the Chlorine and kamiokande II experiment, for a large mixing angle. The difference between the results of the two experiment can be understood on the basis that in the former only ν_e are active, whereas in the latter all the neutrino states contribute to the signal. Our discussion was qualitative in that only two limiting cases (the adiabatic and the sudden solution) have been explored.

iv) Obviously the model predict no $\bar{\nu}_e$ signal from the sun. This is supported by the stringent upper bound on solar $\bar{\nu}_e$ flux from the results

of the Kamioka experiment. ν) The suppression of the neutrino signal with the SSM prediction comes out to be independent of the neutrino energy. Thus we expect the Gallium experiment to give the same modulation as the Chlorine experiment.

APPENDIX A

SPINORS

A generic Dirac field ψ is

$$\psi = \int d\frac{\mathbf{P}}{2p_0(2\pi)^3} e^{-ipx} u^{(\alpha)}(\mathbf{p}) a_{\mathbf{p}}^{(\alpha)} + e^{ipx} v^{(\alpha)}(\mathbf{p}) b_{\mathbf{p}}^{(\alpha)} \quad (A1)$$

where $a_{\mathbf{p}}^{(\alpha)}$ is the creation operator for a particle and $b_{\mathbf{p}}^{(\alpha)}$ for an antiparticle with polarization α , u and v are Dirac quadrispinors.

Creation and annihilation operators are normalized in the following manner

$$\begin{aligned} \{a_{\mathbf{p}}^{(\alpha)}(\mathbf{p}), a_{\mathbf{p}}^{\dagger(\beta)}(\mathbf{q})\} &= (2\pi)^3 \delta_{\alpha\beta} \delta(\mathbf{p} - \mathbf{q}) \\ \{b_{\mathbf{p}}^{(\alpha)}(\mathbf{p}), b_{\mathbf{p}}^{\dagger(\beta)}(\mathbf{q})\} &= (2\pi)^3 \delta_{\alpha\beta} \delta(\mathbf{p} - \mathbf{q}) \end{aligned} \quad (A2)$$

Dirac quadrispinor are normalized in the following manner

$$\begin{aligned} \bar{u}^{(\alpha)}(\mathbf{p}) u^{(\beta)}(\mathbf{p}) &= \delta_{\alpha\beta} 2m \\ \bar{v}^{(\alpha)}(\mathbf{p}) v^{(\beta)}(\mathbf{p}) &= \delta_{\alpha\beta} 2m \end{aligned} \quad (A3)$$

If we impose the Majorana condition $\psi_M = \psi_M^C$ we get

$$\psi_M = \int d\frac{\mathbf{P}}{2p_0(2\pi)^3} e^{-ipx} u^{(\alpha)} a_{\mathbf{p}}^{(\alpha)} + e^{ipx} C \bar{u}^{T(\alpha)} a_{\mathbf{p}}^{\dagger(\alpha)} \quad (A4)$$

where $C = \gamma_0 \gamma_2$ and

$$\gamma_0 = \begin{pmatrix} 0 & 1 \\ 1 & 0 \end{pmatrix} \quad \gamma = \begin{pmatrix} 0 & -\sigma \\ -\sigma & 0 \end{pmatrix} \quad \gamma_3 = \begin{pmatrix} 1 & 0 \\ 0 & -1 \end{pmatrix} \quad (A5)$$

Dealing with neutrinos it is convenient to use spinors in the helicity basis.

Given

$$\chi = \frac{\mathbf{k}}{k}$$

$$\phi^\pm(\mathbf{k}) = \frac{1}{\sqrt{2(1 \mp \chi_3)}} \begin{pmatrix} \pm\chi_1 \mp i\chi_2 \\ 1 \pm \chi_3 \end{pmatrix} \quad (A6)$$

for the Dirac spinor in the helicity basis we get

$$u^\pm(\mathbf{k}) = \frac{1}{\sqrt{2(k_0 + m)}} \begin{pmatrix} (k_0 + m \pm k)\phi^\pm \\ (k_0 + m \pm k)\phi^\mp \end{pmatrix} \quad (A7)$$

Aknowledgments

I am deeply indebted to prof. R. Barbieri who introduced me in the subject of my research and helped me in developing the present thesis.

I wish to aknowledge prof. S. T. Petcov for continuos assistance and suggestions about the thesis.

I am also indebted to prof. G. Fiorentini for many useful discussions and continuos collaboration.

Finally I wish to thank A. Koubek for reading my thesis and U. Aglietti for tecnical support.

- [1] R. Davis et al. Phys. Rev. Lett. 20, 1205 (1968)
- [2] B. Pontecotvo, Chalk River Laboratory Report No PD-205
- [3] J. N. Bahcall, R. K. Ulrich Rev. of Mod. Phys 60, 297 (1988);
J. N. Bahcall et al. Rev. of Mod. Phys. 54, 767 (1982)
- [4] Turk-Chieze Astrophys. J. 335, 415 (1988)
- [5] R. Davis in: proceedings Int. Conf. neutrino '90 (Geneva June 1990),
to appear.
- [6] K. S. Hirata et al. Phys Rev D 38, 448 (1988)
- [7] M. Mori "Recent results form kamiokande-II", proceedings of the third
international workshop on "Neutrino Telescopes", 61 (1991), ed. M. B.
Ceolin.
- [8] R. Davis "the Solar Homestake Experiments and the Variation in the
Solar Neutrino Flux", proceedings of the second international workshop on
"Neutrino Telescopes", 1 (1990), ed. M. B. Ceolin.
- [9] K. S. Hirata et al. Phys. Rev. Lett. 65, 1297 (1990)
- [10] J. N. Bahcall, Rev. of Mod. Phys 50, 881
- [11] B. Pontecorvo, JETP (Sov. Fiz.) 33, 549 (1957);
B. Pontecorvo, JETP (Sov. Fiz.) 34, 247 (1958)
- [12] A. Cisneros, Astrophys. Space Sci. 10, 2634 (1979)
- [13] S. M. Bilenky, Nucl. Phys. B 247, 61 (1984);
B. Kayser, Phys. Rev. D30, 1023
- [13] S. Nussinov, Phys. Lett. B63, 201 (1976)
- [14] R. Barbieri et al., Phys. Lett. B90, 249 (1980);
V. Barger et al., Phys. Rev. Lett. 65, 3084 (1990);
A. Acker et al. Phys Rev. D 43, R1754 (1991)
- [15] L. Wolfenstein, Phys. Rev. D 17, 2639 (1978)
- [16] S. P. Mikheyev and A. Yu Smirnov, Yad. Fiz. 42, 1441 (1985);
S. P. Mikheyev and A. Yu Smirnov, Nuovo Cimento C 9, 17 (1986)

- H. Georgi and L. Randall Phys. Lett. B244, 196 (1990)
- [32] Z. G. Berezhiani, G. Fiorentini, M. Moretti and S. T. Petcov, Phys. Lett. B264, 381 (1991)
- [33] V. Zacek et al., Phys. Rev. D34, 2621 (1986);
G. S. Vidyakin et al., Sov. Phys. JETP 66, 243 (1987)
- [34] R. Barbieri and G. Fiorentini, in: Proc. Second Intern. Workshop on Neutrino telescopes, ed. M. Baldo Ceolin (Venice, 1990)
- [35] K. S. Hirata et al., Phys. Lett. B205, 416 (1988);
D. Casper, in: Proc. Third Intern. Workshop on Neutrino telescopes, ed. M. Baldo Ceolin (Venice, 1991)

